Supporting Information for

Development and Mechanistic Studies of an Optimized Receptor for KMe_3 using Iterative Redesign by Dynamic Combinatorial Chemistry

*Nicholas K. Pinkin, Marcey L. Waters**

Department of Chemistry, CB 3290, University of North Carolina, Chapel Hill, NC 27599

Pages S2-S13 Synthesis of Monomer **N**

Page S14 Peptide Synthesis

Pages S15-S16 Dynamic Combinatorial Libraries

Page S17 Synthesis of $\mathbf{A_2N}$

Pages S18-S23 NMR Characterization of $\mathbf{A_2N}$

Page S24 Extinction Coefficient Determination of $\mathbf{A_2N}$ and $\mathbf{A_2B}$

Page S25 NMR analysis of $\mathbf{A_2N}$ and $\mathbf{A_2B}$ binding to Kme_3

Pages S26-S47 Isothermal Titration Calorimetry binding data

Page S26 Table S1. ITC binding data for the binding of ***meso*$_2$-$\mathbf{A_2N}$** to H3 peptides containing different methylation states of Arg.

Page S27 Table S2. ITC binding data for the binding of each of the $\mathbf{A_2N}$ isomers to various H3 peptides.

Page S28 *meso*$_2$-$\mathbf{A_2N}$ + H3 K9me$_X$

Page S31 *meso*$_2$-$\mathbf{A_2N}$ + H3 R8G K9me$_X$

Page S33 *rac*-$\mathbf{A_2B}$ + H3 K9me$_X$

Page S37 *meso*$_2$-$\mathbf{A_2N}$ + H3 K36me$_X$

Page S38 *meso*$_2$-$\mathbf{A_2N}$ + H3 R8me$_X$

Page S40 *meso*$_1$-$\mathbf{A_2N}$ (+ some *rac*-$\mathbf{A_2N}$) + H3 K9me$_X$

Page S44 *rac*-$\mathbf{A_2N}$ (+ some *meso*$_1$-$\mathbf{A_2N}$) + H3K9me$_X$

Page S48 Gas phase minimized structures of meso1- $\mathbf{A_2N}$ and meso2- $\mathbf{A_2N}$ in the absence and presence of butyl trimethyl ammonium.

Synthesis of Monomer N

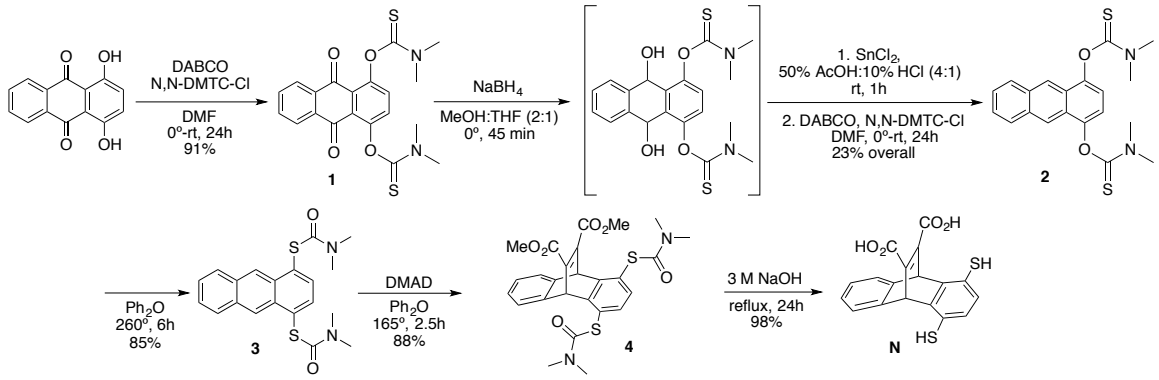

Scheme S1: Synthesis of monomer **N**.

1,4-bis((dimethylcarbamothioyl)oxy)-anthraquinone 1: Quinizarin (1 g, 4.17 mmol) was dissolved in 25 mL anhydrous DMF under a nitrogen atmosphere. The solution was cooled to 0 °C and DABCO (2.802 mg, 24.99 mmol) was added in portions. To the resulting suspension, N,N-dimethylthiocarbamoyl chloride (3.094 g, 24.99 mmol) was added and the solution was allowed to stir at room temperature overnight. Pouring the reaction mixture into 15 mL of H_2O precipitated the product, which was washed with water and cold ethyl acetate to yield the pure product, a yellow solid (1.57 g, 91 % yield). ^{1}H NMR ($CDCl_3$, 600 MHz): δ = 8.139 (m, 2H, C-H), 7.716 (m, 2H, C-H), 7.449 (s, 2H, C-H), 3.535 (s, 6H, N-CH_3), 3.523 (s, 6H, N-CH_3). ^{13}C NMR ($CDCl_3$, 150 MHz): δ = 186.88, 181.73, 151.10, 133.97, 133.59, 131.93, 127.02, 126.79, 43.54, 39.37. MS (calculated): 437.07 $[M+Na]^+$. MS (observed, ESI+): 437.03 $[M+Na]^+$

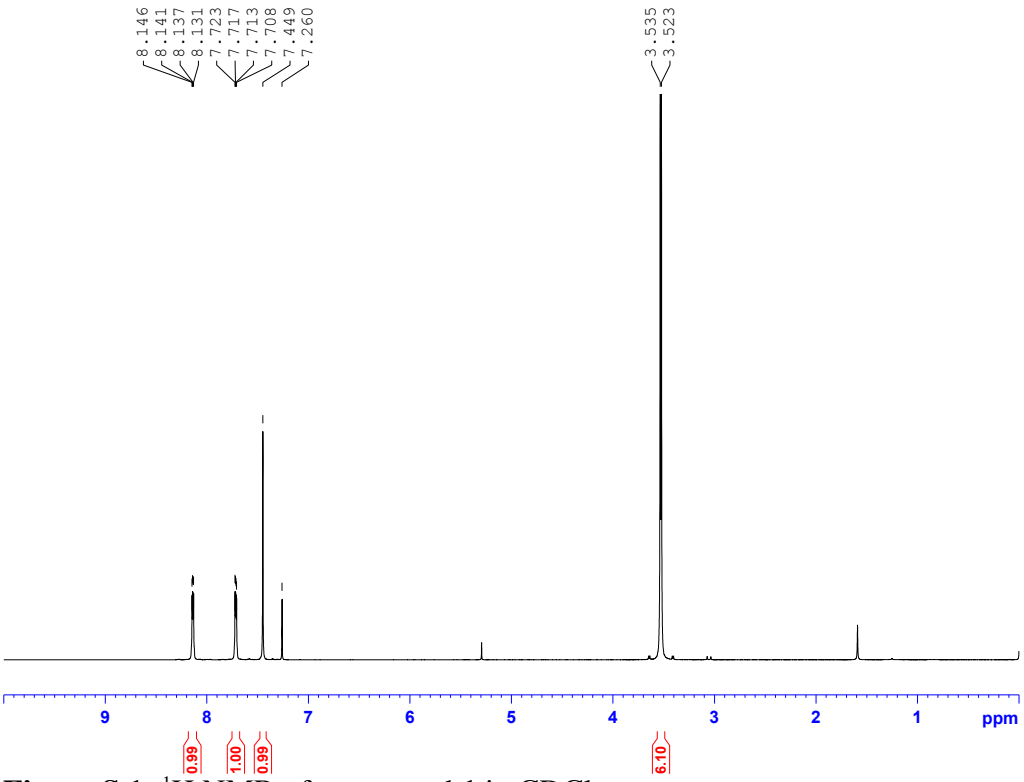

Figure S 1: ^{1}H NMR of compound **1** in $CDCl_3$.

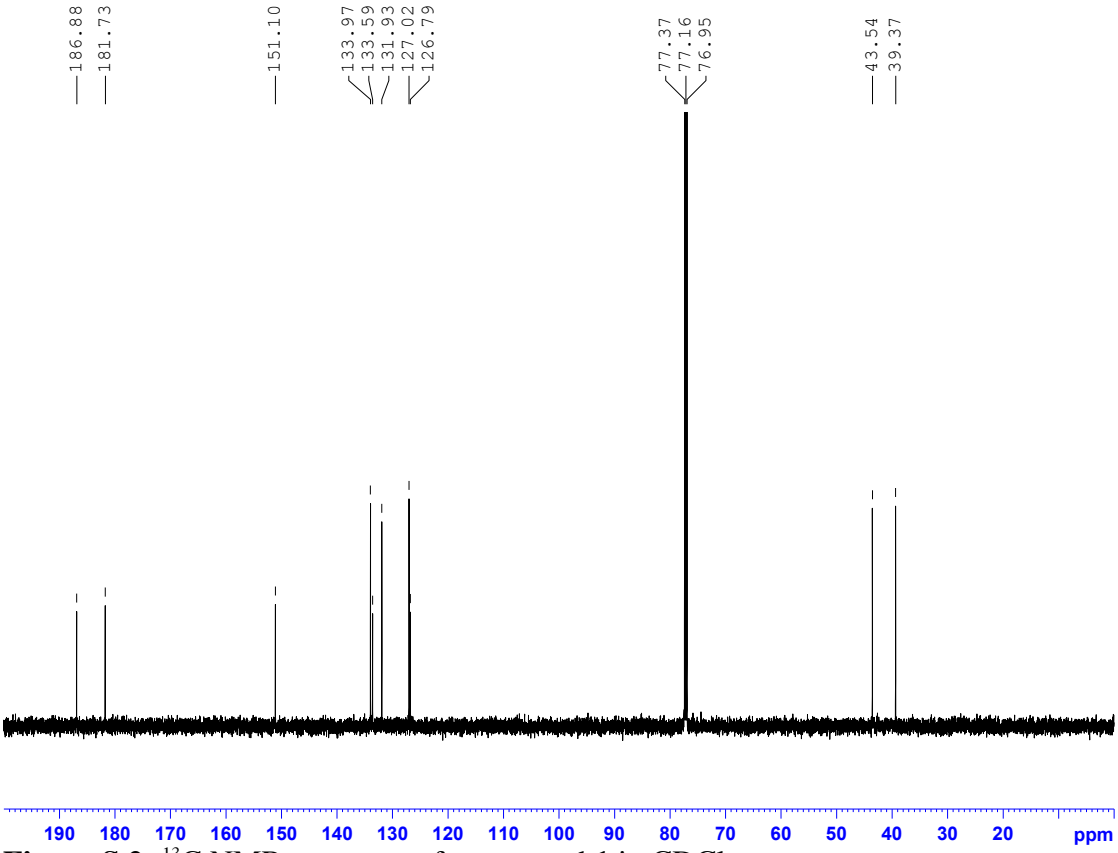

Figure S 2: ^{13}C NMR spectrum of compound **1** in $CDCl_3$.

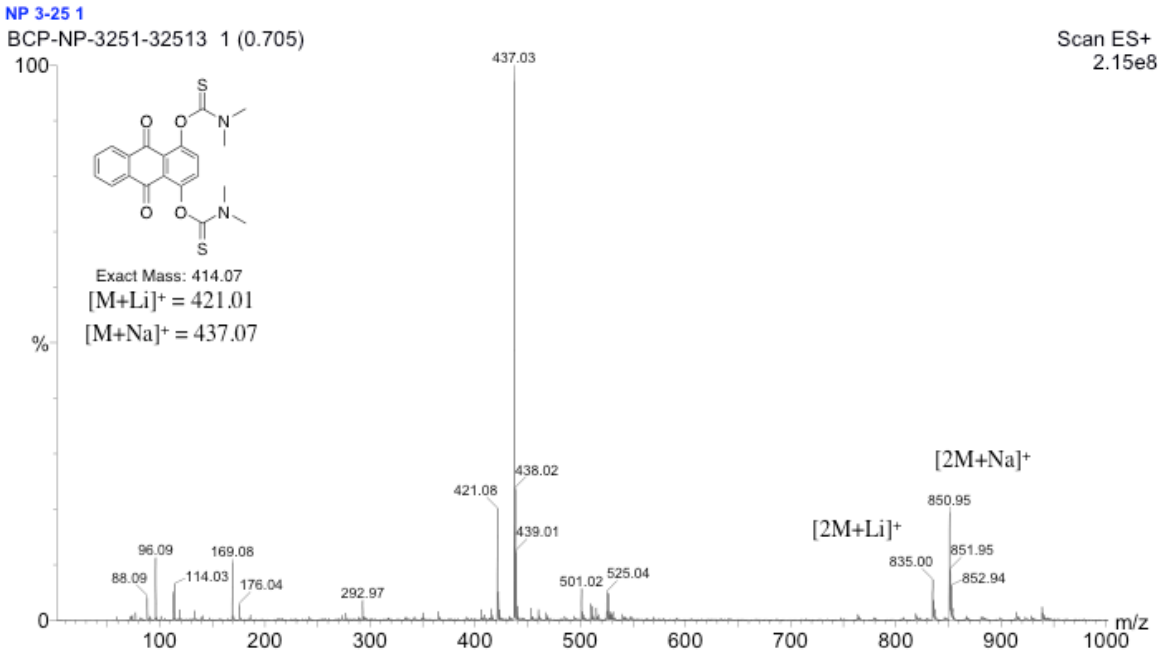

Figure S 3. ESI(+) mass spectrum of compound **1**.

1,4-bis((dimethylcarbamothioyl)oxy)-anthracene 2: Compound **1** (500 mg, 1.21 mmol) was dissolved in a 2:1 mixture of MeOH:THF (30 mL) and cooled to 0 °C under nitrogen atmosphere. $NaBH_4$ (273.8 mg, 7.24 mmol) was added and the reaction was allowed to react for 30 minutes. The reaction was then quenched by acidification with acetic acid. The intermediate diol was isolated by extraction between ethyl acetate and water, followed by washing of the combined organic extracts with 1 M $NaHCO_3$ and brine. Evaporation of the organic extracts yields an orange solid (480 mg, 98% yield). Due to the instability of this intermediate diol to oxidation, the crude product is taken on without purification through a reductive elimination to give the stable anthracene. This was accomplished by slowly dripping the quenched $NaBH_4$ reaction mixture into a solution of tin (II) chloride (1.147 g, 6.05 mmol) in 50% AcOH (20 mL) and 10% HCl (5 mL) that had been degassed with nitrogen for 2 hours. This solution was allowed to stir at room temperature for 2 hours. When the reaction was complete, it was poured over a bed of silica and dichloromethane was used to wash all products off of the silica, leaving any tin salts behind. The products were extracted into dichloromethane, and the organic extracts washed with 1 M $NaHCO_3$ and brine. The organic layer was collected and dried with $MgSO_4$, then evaporated to yield a dark orange solid. Due to the observation of a small degree of deprotection of the thiocarbamate group, the solid was dissolved in DMF (20 mL) and treated with DABCO (1.0 g, 8.92 mmol) and DMTC-Cl (1.10 g, 8.92 mmol) and allowed to react at room temperature overnight. The products were precipitated by pouring the reaction mixture into 200 mL of H_2O and were isolated by filtration. The product was purified from the resulting red-brown solid by column chromatography (CH_2Cl_2). Removal of solvent yields a yellow crystalline solid (107 mg, 23% overall yield). ^{1}H NMR ($CDCl_3$, 400 MHz) δ = 8.382 (s, 2H, C-H), 7.989 (m, 2H, C-H), 7.466 (m, 2H, C-H), 7.209 (s, 2H, C-H), 3.588 (s, 12H, N-CH_3). ^{13}C NMR ($CDCl_3$, 100 MHz): δ = 188.05, 147.86, 132.02, 128.66, 126.78, 126.28, 121.32, 117.85, 43.62, 39.11. MS (calculated): 407.10 $[M+Na]^+$. MS (observed, ESI+): 407.05 $[M+Na]^+$

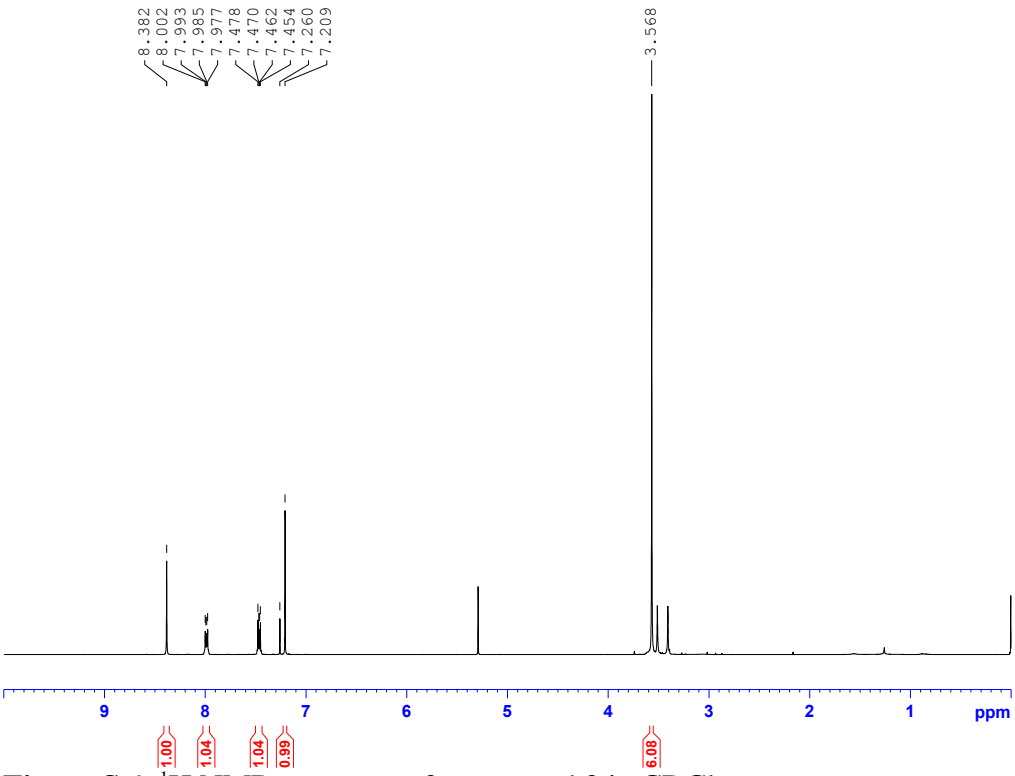

Figure S 4. ^{1}H NMR spectrum of compound **2** in $CDCl_3$.

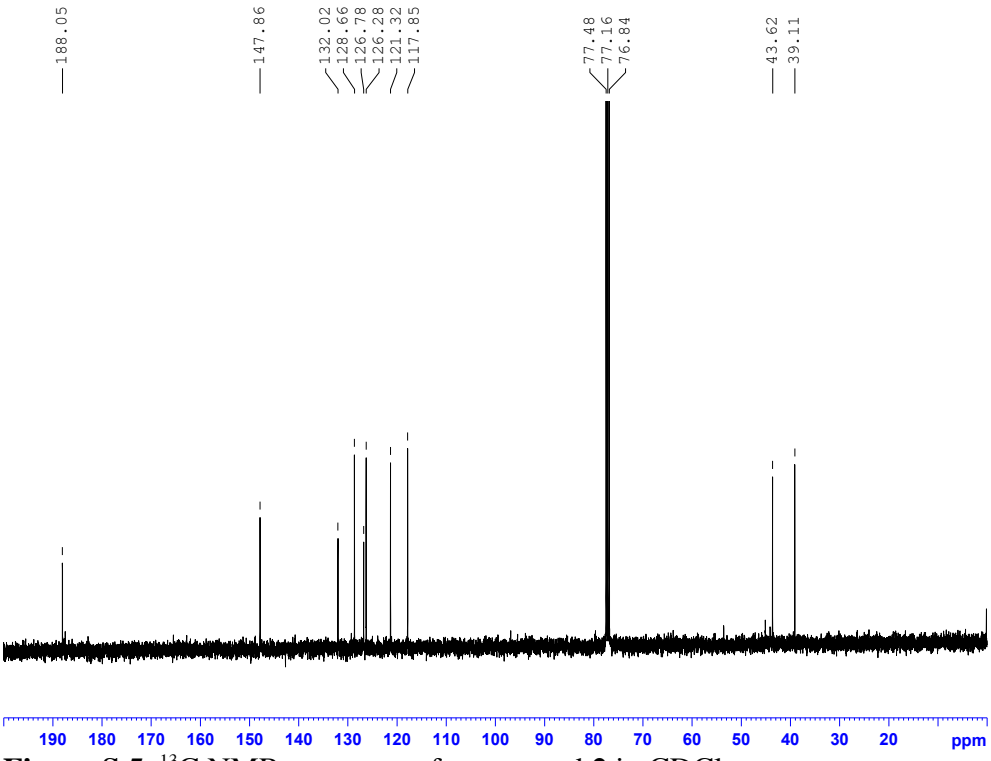

Figure S 5. ^{13}C NMR spectrum of compound **2** in $CDCl_3$.

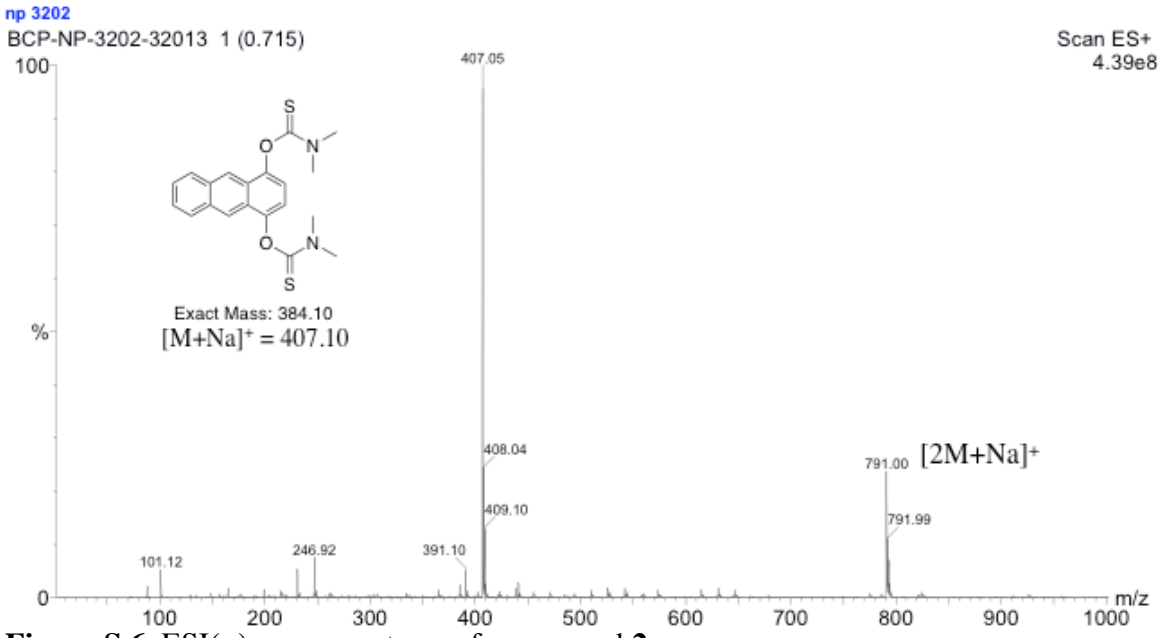

Figure S 6. ESI(+) mass spectrum of compound **2**.

1,4-bis((dimethylcarbamoyl)thio)-anthracene 3: Compound **2** (85 mg, 0.221 mmol) was dissolved in dry diphenyl ether (10 mL) under nitrogen atmosphere. This solution was slowly heated to 260 °C, then allowed to stir for six hours. The solution was then cooled to room temperature and the product recovered from the diphenyl ether by running over a plug of silica using pure hexanes. After the diphenyl ether eluted, increasing amounts of ethyl acetate were used to elute the product. (60 mg, 71 % yield). ^{1}H NMR ($CDCl_3$, 400 MHz): δ = 8.971 (s, 2H, C-H), 8.061 (m, 2H, C-H), 7.822 (s, 2H, C-H), 7.491 (m, 2H, C-H), 3.281 (s, 6H, N-CH_3), 3.036 (s, 6H, N-CH_3). ^{13}C NMR ($CDCl_3$, 150 MHz): δ = 166.15, 135.43, 133.23, 132.32, 129.60, 128.63, 126.15, 125.77, 37.26. MS (calculated): 407.10 $[M+Na]^+$. MS (observed, ESI+): 407.05 $[M+Na]^+$

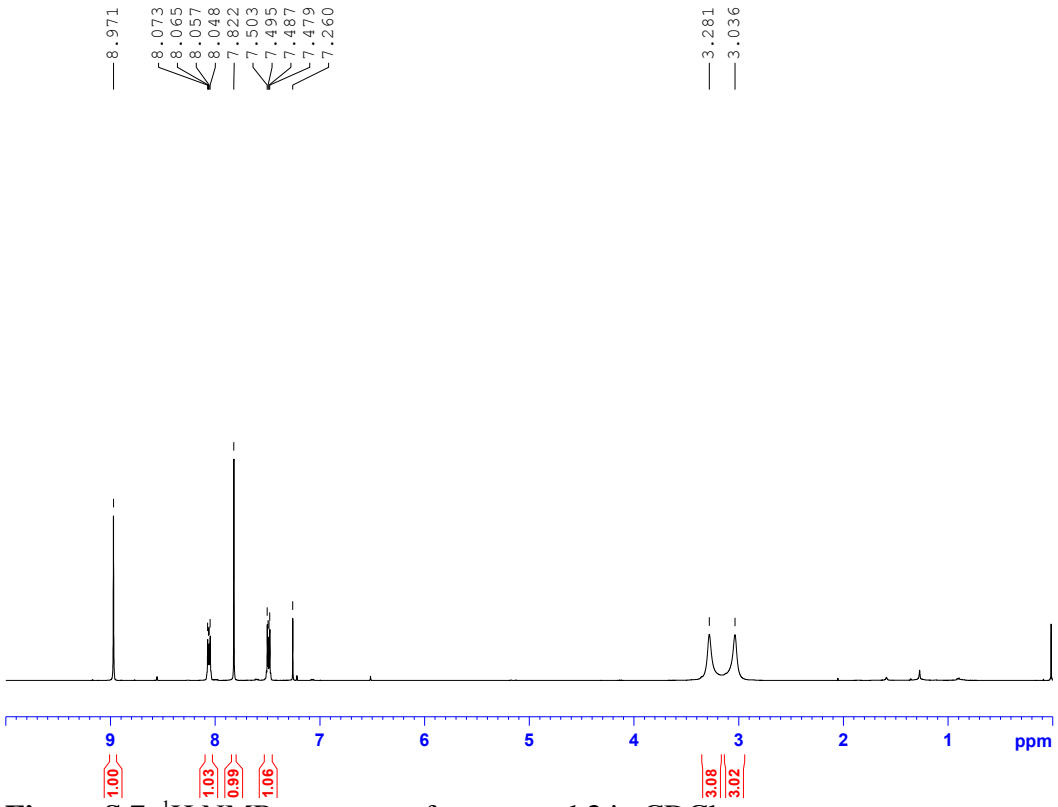

Figure S 7. ^{1}H NMR spectrum of compound **3** in $CDCl_3$.

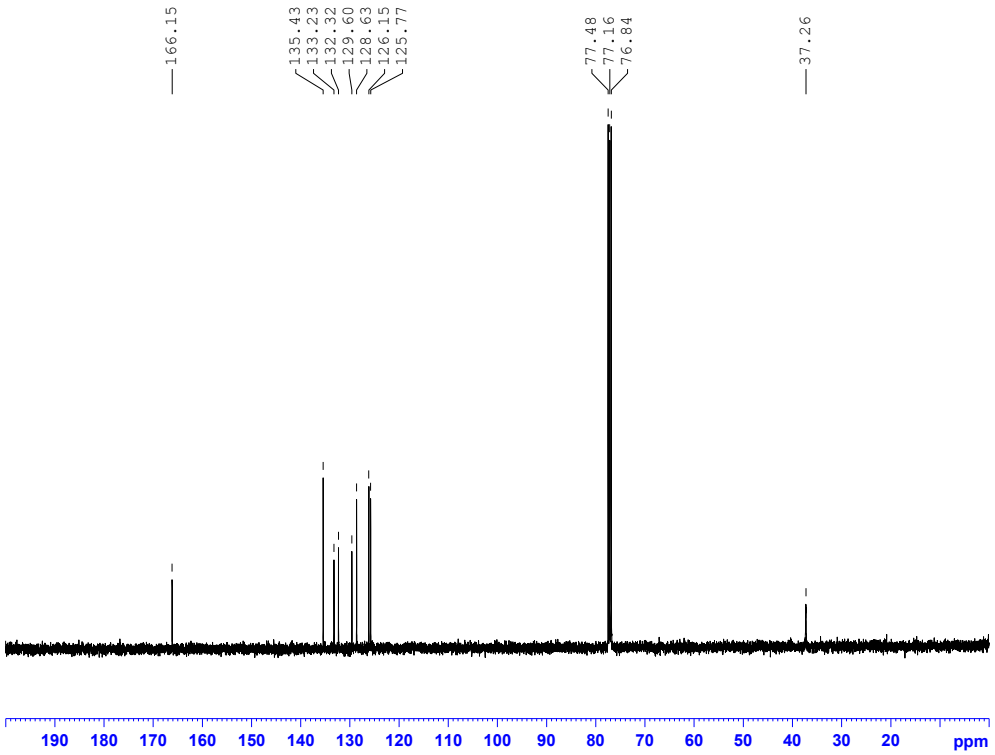

Figure S 8. ^{13}C NMR spectrum of compound **3** in $CDCl_3$.

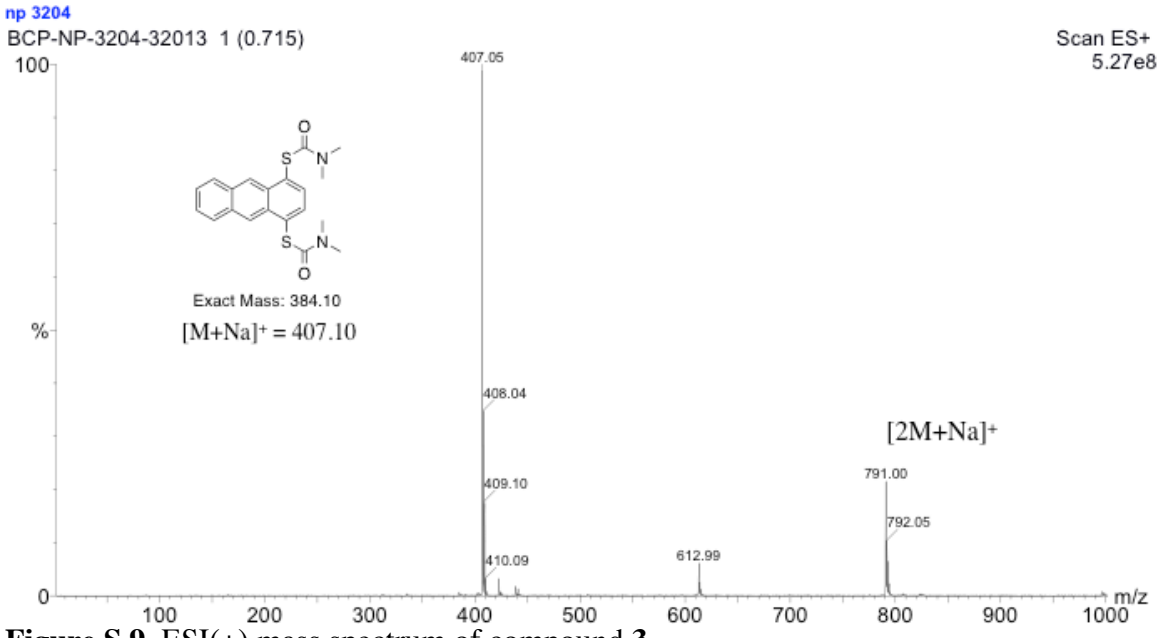

Figure S 9. ESI(+) mass spectrum of compound **3**.

(9R,10S)-dimethyl-1,4-bis((dimethylcarbamoyl)thio)-9,10-dihydro-9,10-ethenoanthracene-11,12-dicarboxylate 4: Compound **3** (80 mg, 0.208 mmol) and dimethyl acetylene dicarboxylate (DMAD, 0.135 mL 1.09 mmol) were dissolved in 6 mL diphenyl ether under nitrogen atmosphere. This solution was slowly heated to 165 °C and allowed to stir at this temperature for 2.5 hours. After cooling to room temperature, the product was isolated by running the reaction mixture over a bed of silica with pure hexanes until the diphenyl ether had completely eluted, and then increasing the solvent polarity with ethyl acetate until the product eluted. (96.7 mg, 88.2 % yield) ^{1}H NMR ($CDCl_3$, 600 MHz): δ = 7.375 (m, 2H, C-H), 7.150 (s, 2H, C-H), 7.013 (m, 2H, C-H), 5.908 (s, 2H, C-H), 3.758 (s, 6H, OCH_3), 3.190 (s, 6H, NCH_3), 3.027 (s, 6H, NCH_3). ^{13}C NMR ($CDCl_3$, 150 MHz): δ = 166.22, 165.33, 149.38, 147.09, 143.35, 132.86, 126.03, 125.64, 124.54, 52.34, 51.54, 37.15. MS (calculated): 549.12 $[M+Na]^+$. MS (observed, ESI+): 549.13 $[M+Na]^+$

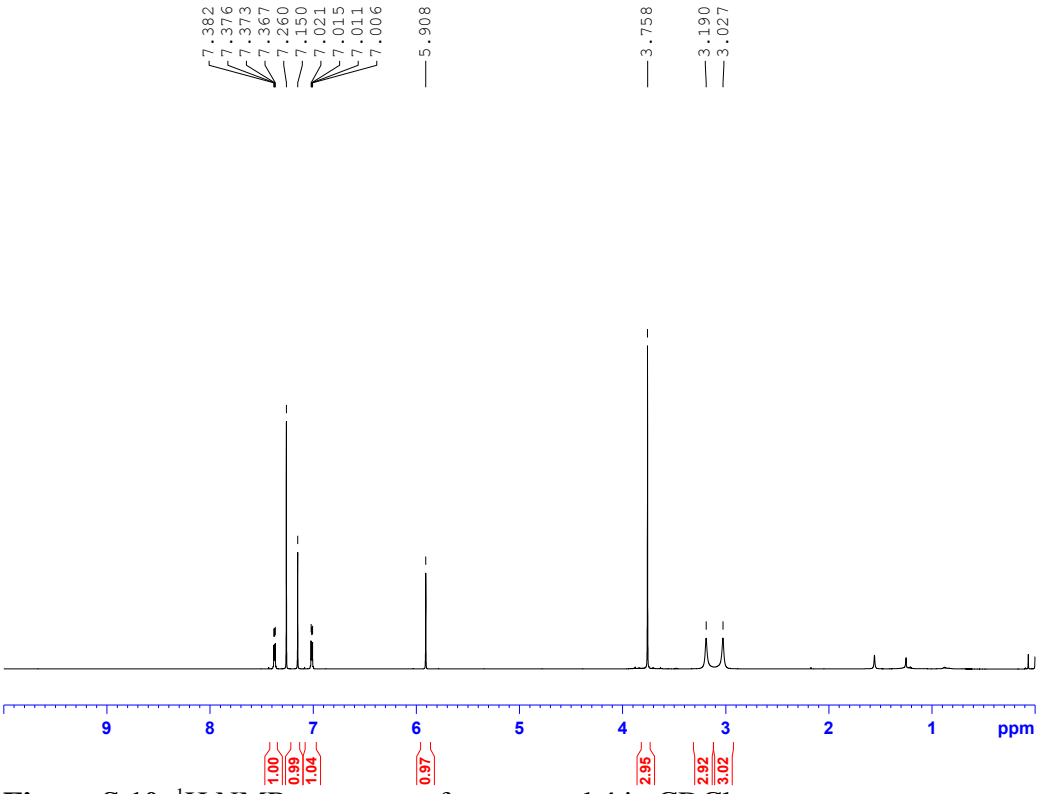

Figure S 10. ^{1}H NMR spectrum of compound **4** in $CDCl_3$.

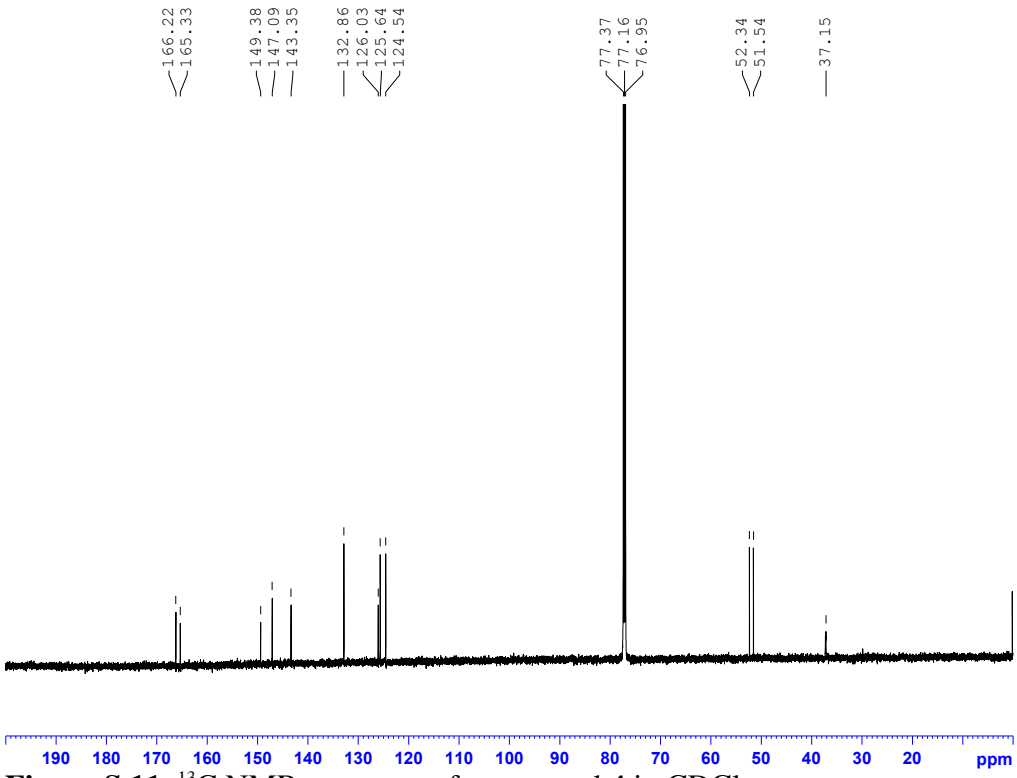

Figure S 11. ^{13}C NMR spectrum of compound **4** in $CDCl_3$.

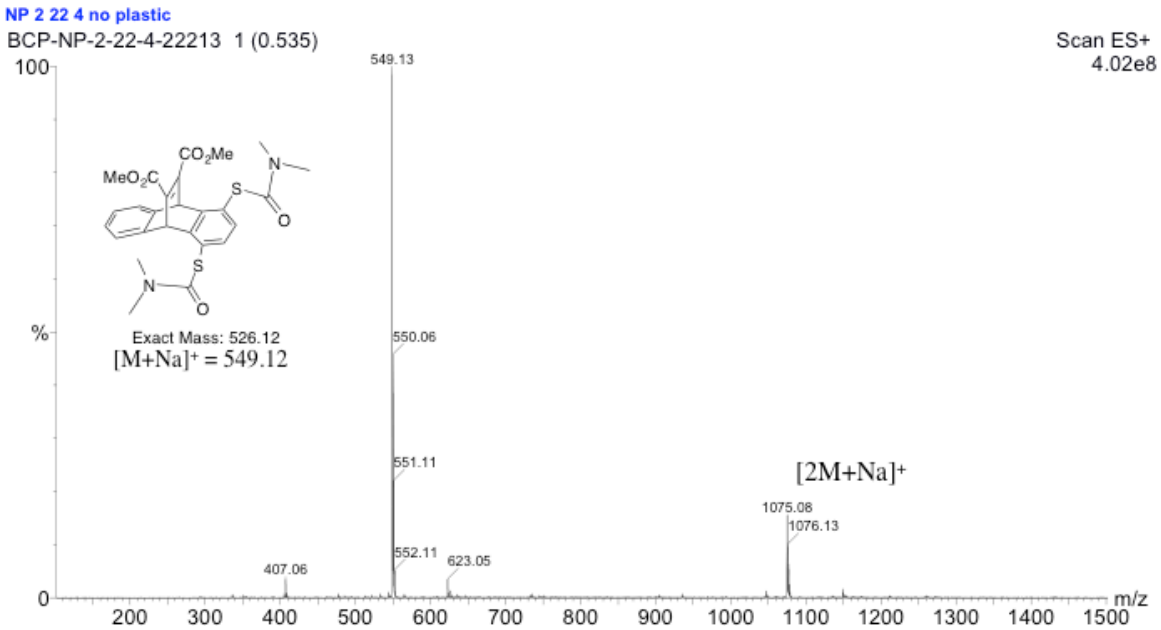

Figure S 12. ESI(+) mass spectrum of compound **4**.

(9R,10S)-1,4-dimercapto-9,10-dihydro-9,10-ethenoanthracene-11,12-dicarboxylic acid 5: Compound **4** (96.7 mg, 0.184 mmol) was measured into a round bottom flask with reflux adapter and was swept with nitrogen for at least an hour. To it was added 3 mL of degassed 6 N NaOH and 3 mL of degassed H_2O. This solution was slowly brought to reflux and was allowed to react overnight. The reaction was then cooled to room temperature, diluted with 6 mL of degassed H_2O, and then acidified with concentrated HCl. The precipitate was isolated by centrifugation at 5000 rpm for 20 minutes. This was repeated two times with slightly acidic water to remove salts. The remaining solid was then dissolved into methanol and centrifuged one more time to precipitate any remaining salts and the methanol poured off and evaporated to yield the final compound, a tan solid (54 mg, 80 % yield). ^{1}H NMR (CD_3OD, 600 MHz): δ = 7.444 (m, 2H, C-H), 7.074 (m, 2H, C-H), 6.949 (s, 2H, C-H), 6.016 (s, 2H, C-H). ^{13}C NMR (CD_3OD, 150 MHz): δ =168.53, 149.15, 145.19, 144.67, 129.54, 126.80, 125.36, 125.06. MS (calculated): 355.01 $[M-H]^-$. MS (observed, ESI-): 355.03 $[M-H]^-$

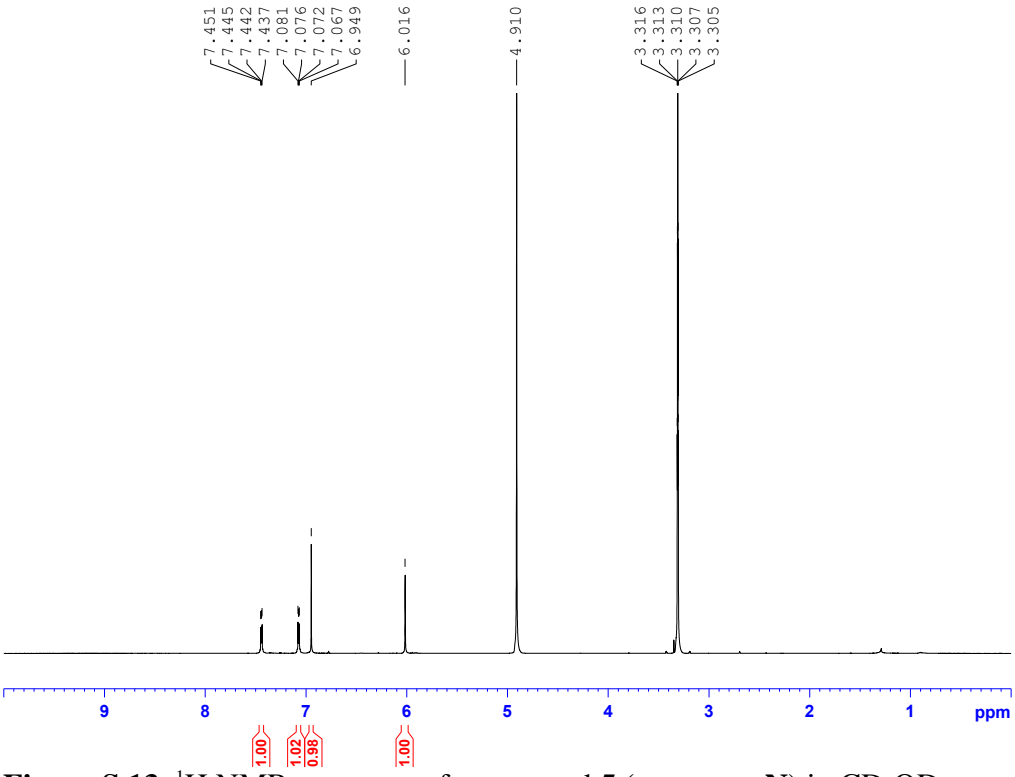

Figure S 13. ^{1}H NMR spectrum of compound **5** (monomer **N**) in CD_3OD.

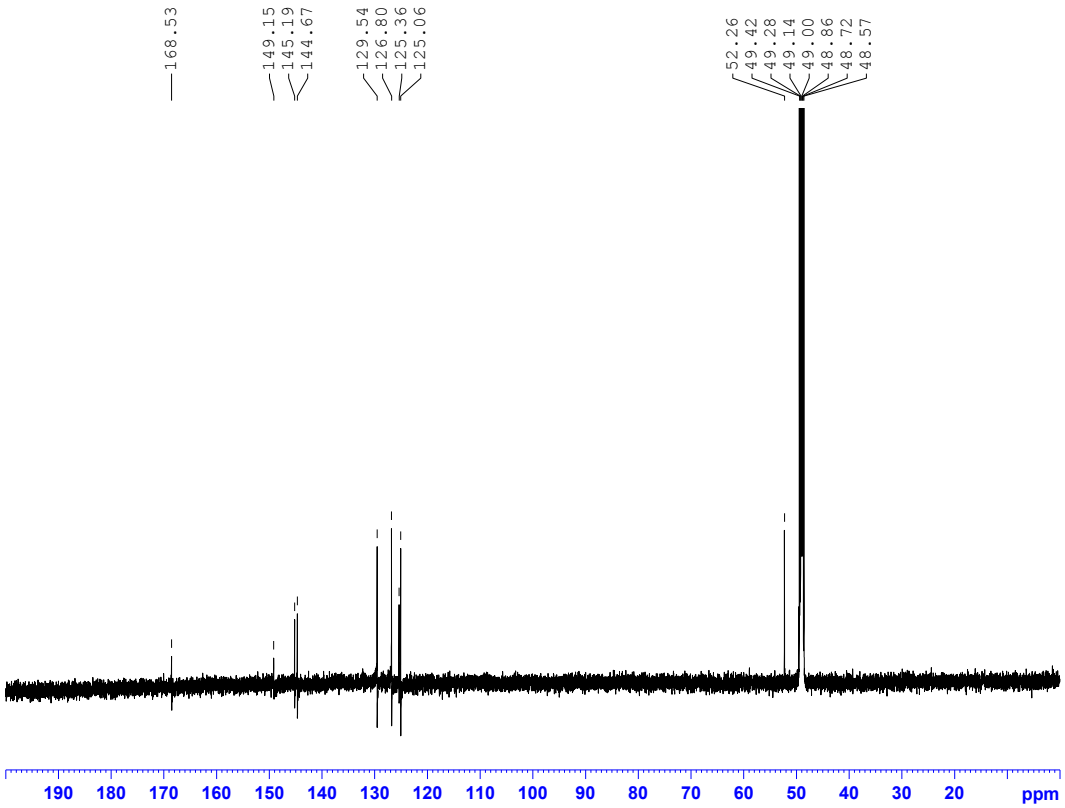

Figure S 14. ^{1}H NMR spectrum of compound **5** (monomer **N**) in CD_3OD.

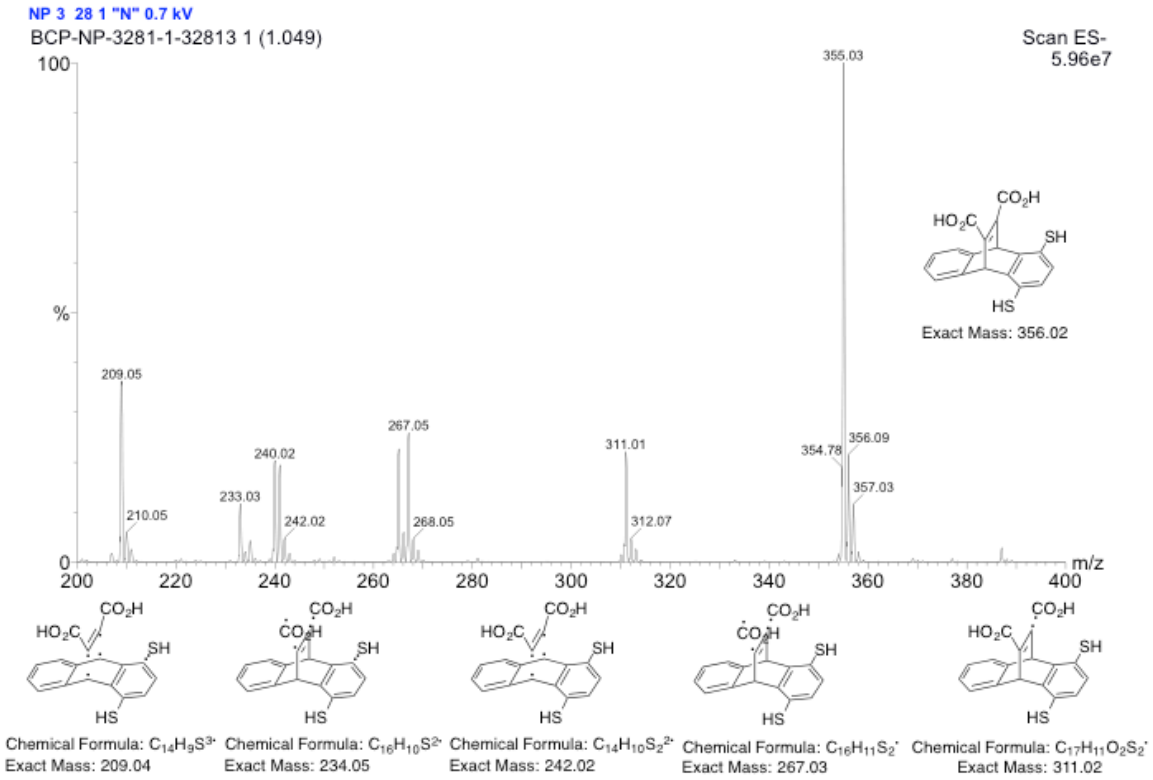

Figure S 15. ESI(-) mass spectrum of compound **5** (monomer **N**).

Peptide Synthesis: All peptide synthesis was performed on a Tetras Peptide Synthesizer using CLEAR-Amide resin from Peptides International. Peptides were synthesized on a 0.6 mmol scale. All amino acids with functionality were protected during synthesis. Coupling reagents were HOBt/HBTU in DMF. All peptides were acylated at the N-terminus with a solution of 5% acetic anhydride and 6% 2,6-lutidine in DMF. Cleavage was performed by hand with a cocktail of 95% TFA/2.5% triisopropylsilane/2.5% H_2O for 3 hours. Peptides were purified by semipreparative reverse-phase HPLC on a C18 column at a flow rate of 4 mL/min. Peptides were purified with a linear gradient of A and B (A: 95% H_2O/5% CH_3CN with 0.1% TFA, B: 95% CH_3CN/5% H_2O with 0.1 % TFA) and elution was monitored at 214 nm. Once purified, peptides were lyophilized to powder and characterized by ESI-MS.

Methylated peptides were synthesized with either 2 equivalents of Fmoc-Lys(Boc)(Me)-OH purchased from BaChem or Fmoc-Lys$(Me)_2$-OH HCl purchased from Anaspec and coupled for 5 hours. The trimethyllysine containing peptides were synthesized by reacting corresponding dimethylated peptides (0.06 mmol scale) prior to cleavage from the resin with MTBD (10 equil) and methyl iodide (10 equil) in DMF (5 mL) for 5 hours with bubbling N_2 in a peptide flask. After washing the resin with DMF and CH_2Cl_2 and drying, the peptide was cleaved as normal.

Dynamic Combinatorial Chemistry:

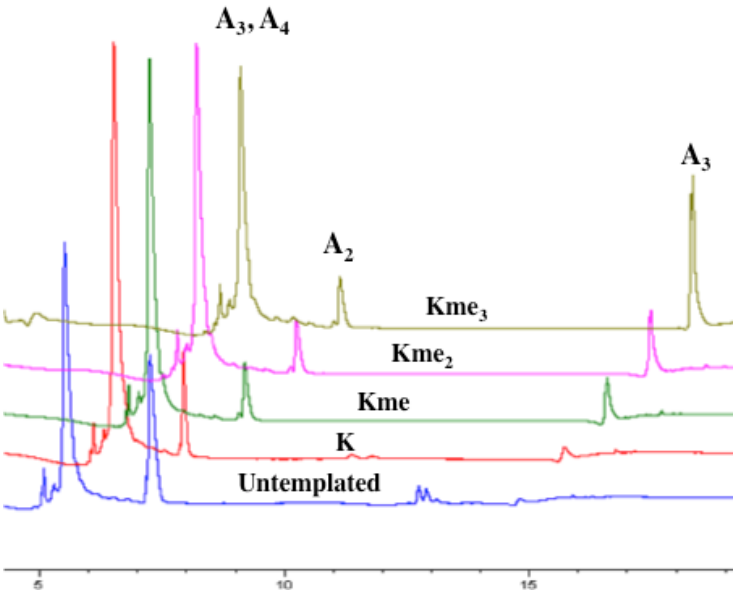

Figure S 16. Overlaid HPLC traces of the day 12 DCLs containing 2.5 mM **A** and 2.5 mM guest. $\mathbf{A_3}$ is observed to amplify in the presence of Kme_3.

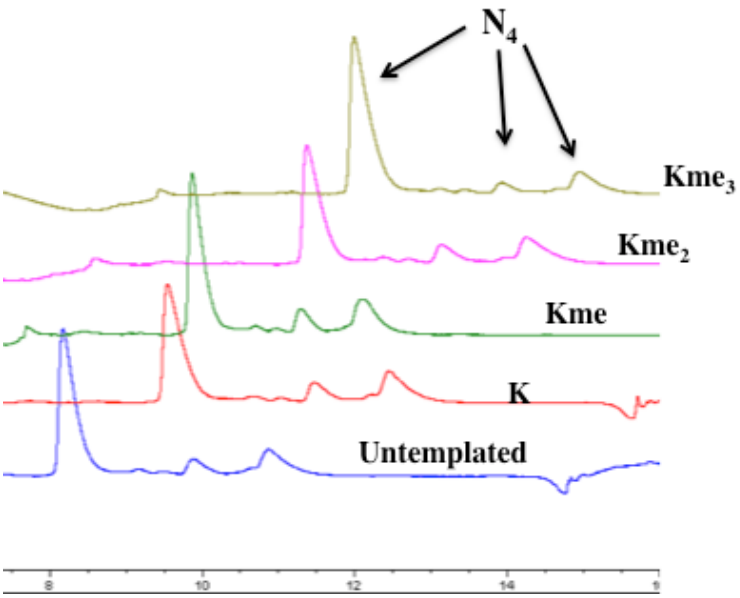

Figure S 17. Overlaid HPLC traces of the day 12 DCLs containing 2.5 mM **N** and 2.5 mM guest. No species are amplified in the presence of the peptide guests compared to the untemplated library. $\mathbf{N_4}$ was the only species observed and the variation in retention time is contributed to possible structural isomers of $\mathbf{N_4}$.

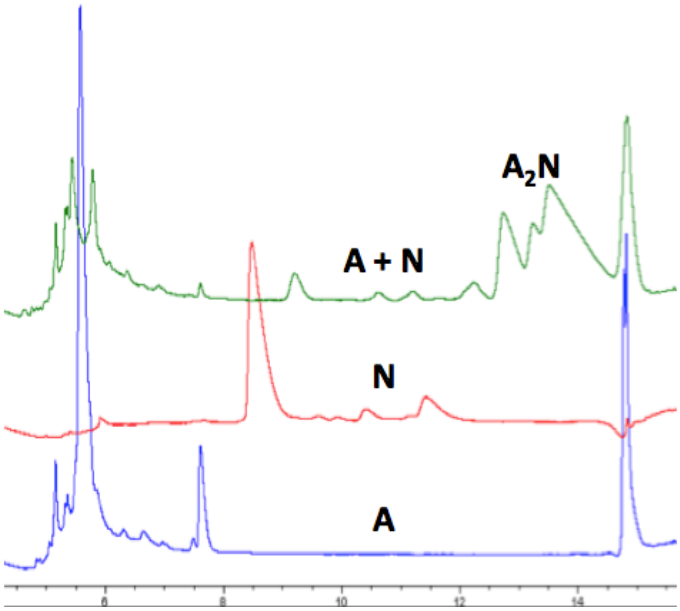

Figure S 18. Overlaid day 12 traces of the DCLs containing Ac-Kme_3GGL-NH_2 and the indicated monomers. Although initial identification of the amplified trimers in the library of **A** and **N** was complicated by the identical masses of the monomers, overlaid traces indicated that the new species must incorporate both monomers.

Synthesis of A_2N: Preparative scale DCLs were set up using acetylcholine chloride (AcCh) as a guest to template the formation of **A_2N**. AcCh was used as the template because of its low cost compared to a Kme_3 peptide and its ability to drive the formation of **A_2N** when used in excess in a prep library. Libraries were set up in 50 mM sodium borate buffer (pH 8.5) to be a final concentration of 2 mM in guests **A** and **N** and 10 mM in acetylcholine. After equilibration at room temperature for 5 days, **A_2N** was isolated by semi-preparative HPLC (solvent A: 10 mM NH_4OAc in H_2O; solvent B: 10 mM NH_4OAc in 9:1 CH_3CN:H_2O) using the gradient: 0-39% B from 0-1 min, then 39-41% B from 1-20 with a flow rate of 4.0 mL/min. Under these optimized conditions, *meso*$_2$-**A_2N** can be purely isolated at 11.3 min (23% isolated yield), but *meso*$_1$-**A_2N** and *rac*-**A_2N** nearly co-elute at 10.1 min (combined 21.5% isolated yield). Isolated fractions are lyophilized to yield white powders and are stored under nitrogen.

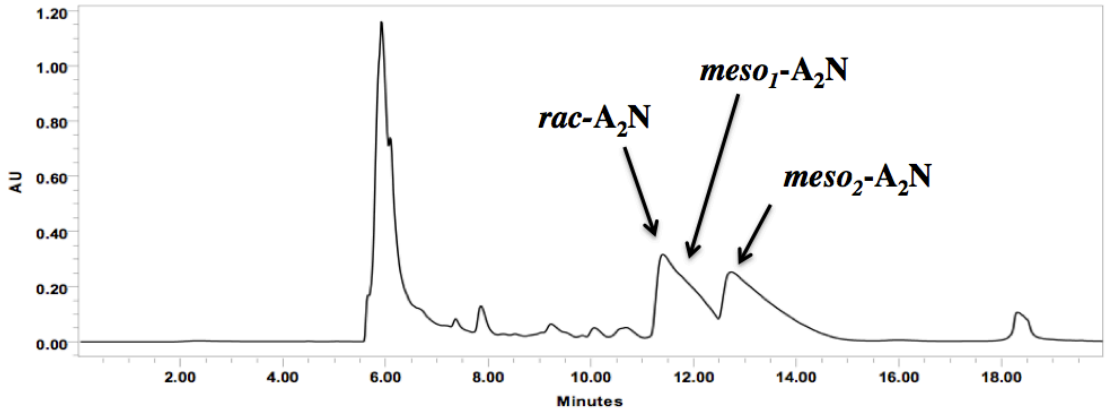

Figure S 19. Semi-preparative HPLC trace of a preparative scale **A_2N** library monitored at 254 nm.

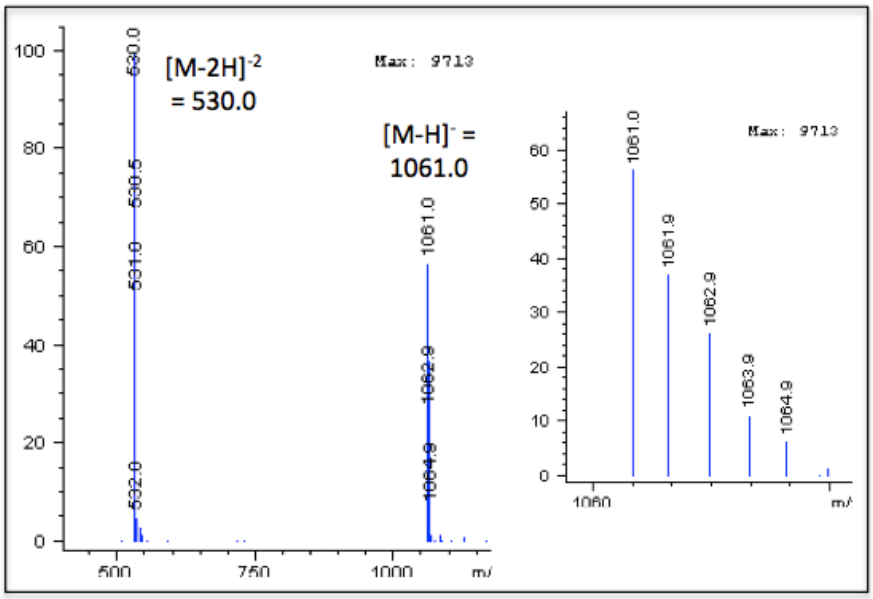

Figure S 20. Mass spectrum of **A_2N** (-ESI)

NMR Characterization of A_2N: Structural characterization of the three isomers of **A_2N** was carried out in CD_3OD on a Bruker 500 MHz NMR instrument unless otherwise stated. Peak assignments were made for the two *meso* isomers using a combination of TOCSY, COSY, and ROESY. Due to the complexity of the *rac*-**A_2N** spectrum, and the inability to obtain a high enough quantity of a pure sample, peak assignments were not made. Variable temperature experiments revealed the spectra of the receptors to sharpen with increasing temperature, and 313 K was chosen as the temperature to assign chemical shifts and obtain 2D spectra. A spectrum of *meso*$_2$-**A_2N** was obtained in D_2O, but even at 323 K peaks did not sharpen as cleanly as was observed in CD_3OD.

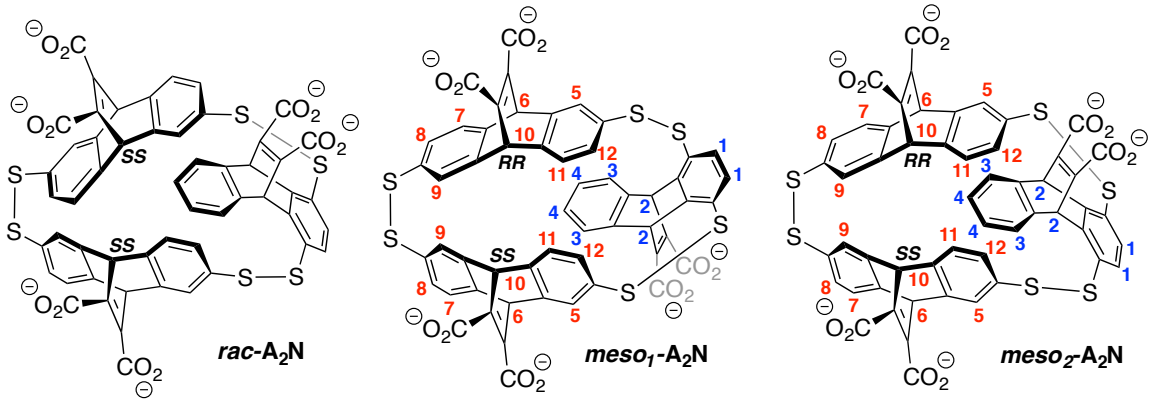

Figure S 21. Structures of the three isomers of **A_2N** that are supported by NMR characterization in CD_3OD. Peak assignments were only made for the two *meso* isomers of the receptor. Due to the symmetry of the *meso* isomers, all peaks represent two identical protons.

Meso$_2$-**A$_2$N**:

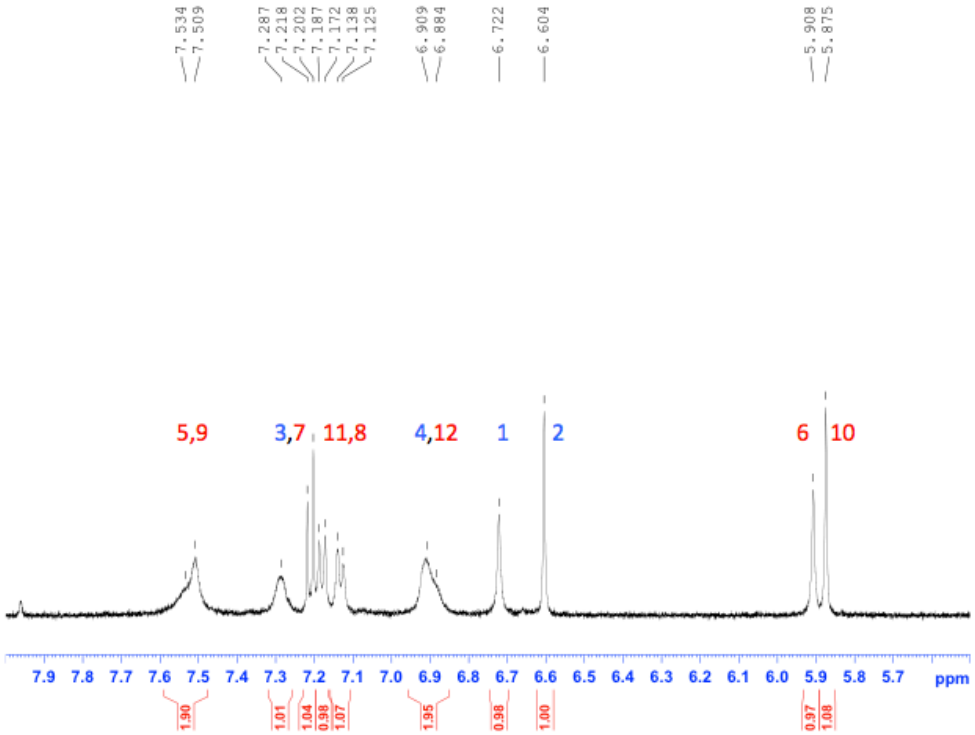

Figure S 22. ^{1}H NMR spectrum of *meso*$_2$-**A$_2$N** in CD_3OD at 313K. δ = 7.534 (broad s, 2H, C-H), 7.509 (s, 2H, C-H), 7.287 (broad s, 2H, C-H), 7.210 (d, 2H, C-H), 7.180 (d, 2H, C-H), 7.132 (d, 2H, C-H), 6.909 (s, 2H, C-H), 6.884 (broad s, 2H, C-H), 6.772 (s, 2H, C-H), 6.604 (s, 2H, C-H), 5.908 (s, 2H, C-H), 5.875 (s, 2H, C-H).

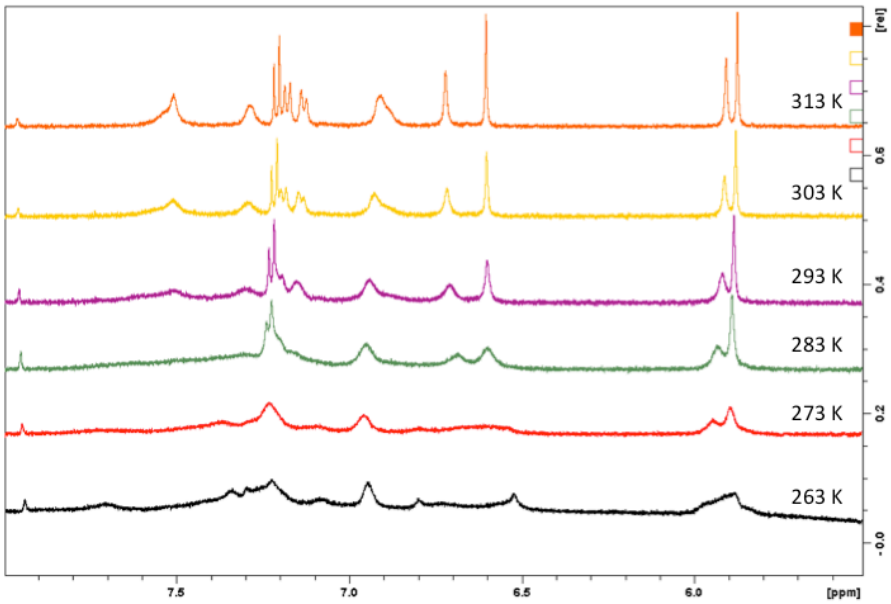

Figure S 23. Impact of temperature on the ^{1}H NMR spectrum of *meso*$_2$-**A$_2$N** in CD_3OD.

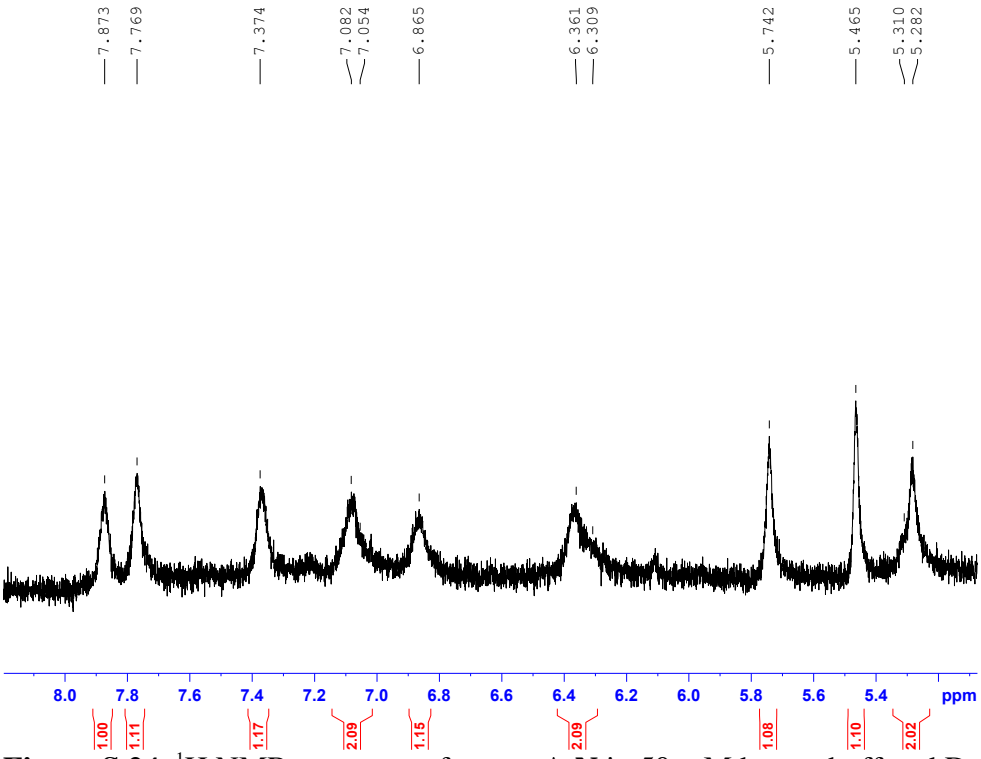

Figure S 24. ^{1}H NMR spectrum of *meso*$_2$-**A$_2$N** in 50 mM borate buffered D_2O (pH 8.67) at 323K. δ = 7.873 (s, 2H, C-H), 7.769 (s, 2H, C-H), 7.374 (s, 2H, C-H), 7.082 (s, 2H, C-H), 7.054 (broad s, 2H, C-H), 6.865 (s, 2H, C-H), 6.361 (s, 2H, C-H), 6.309 (broad s, 2H, C-H), 5.742 (s, 2H, C-H), 5.465 (s, 2H, C-H), 5.310 (s, 2H, C-H), 5.282 (s, 2H, C-H).

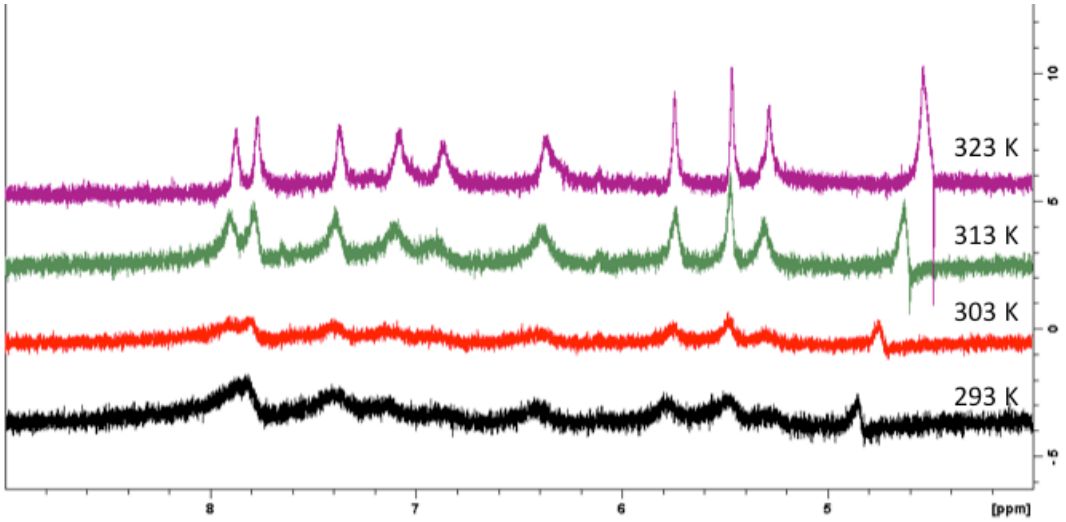

Figure S 25. Impact of temperature on the ^{1}H NMR spectrum of *meso*$_2$-**A$_2$N** in 50 mM borate buffered D_2O (pH 8.67). 2D NMR characterization was not pursued in D_2O due to the persistent broadness of peaks as high as 323 K.

Meso$_1$ **A$_2$N**: *Due to co-elution with *rac*-**A$_2$N** during HPLC purification, NMR spectra represent a mixture of the two isomers.

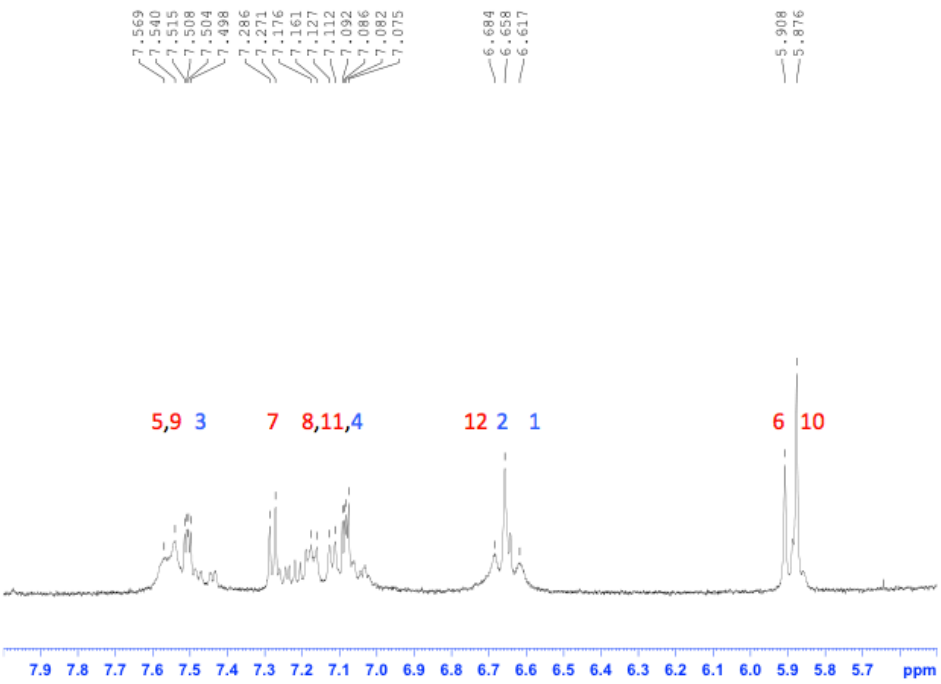

Figure S 26. ^{1}H NMR spectrum of a mixture of *meso*$_1$-**A$_2$N** (major species) and *rac*-**A$_2$N** (minor species) in CD_3OD at 313 K. δ = 7.569 (s, 2H, C-H), 7.540 (s, 2H, C-H), 7.506 (m, 2H, C-H), 7.279 (d, 2H, C-H), 7.169 (d, 2H, C-H), 7.120 (d, 2H, C-H), 7.084 (m, 2H, C-H), 6.684 (s, 2H, C-H), 6.658 (s, 2H, C-H), 6.617 (s, 2H, C-H), 5.908 (s, 2H, C-H), 5.876 (s, 2H, C-H).

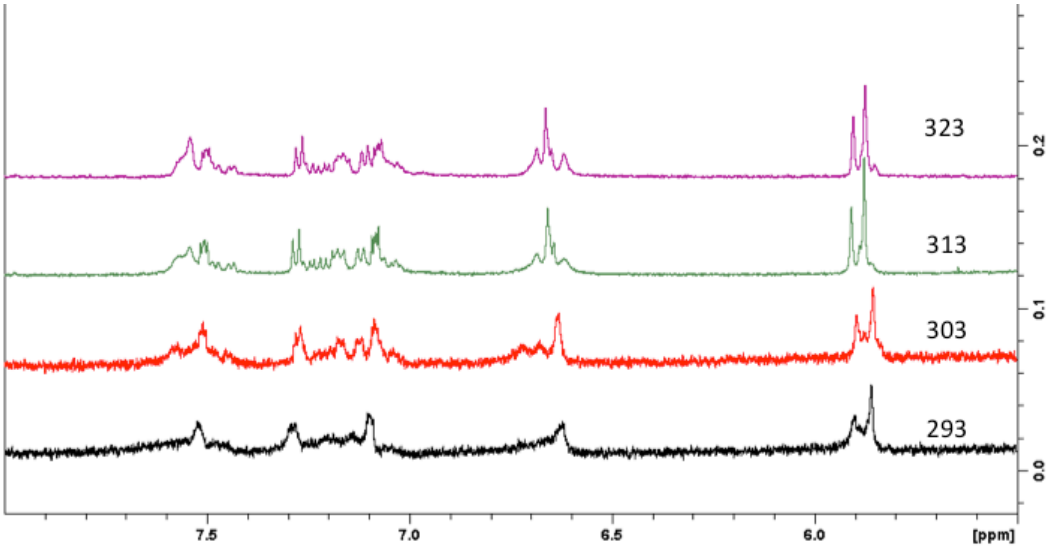

Figure S 27. Impact of temperature on the ^{1}H NMR of a mixture of *meso*$_1$-**A$_2$N** (major) and *rac*-**A$_2$N** (minor) in CD_3OD.

Rac-**A_2N**:

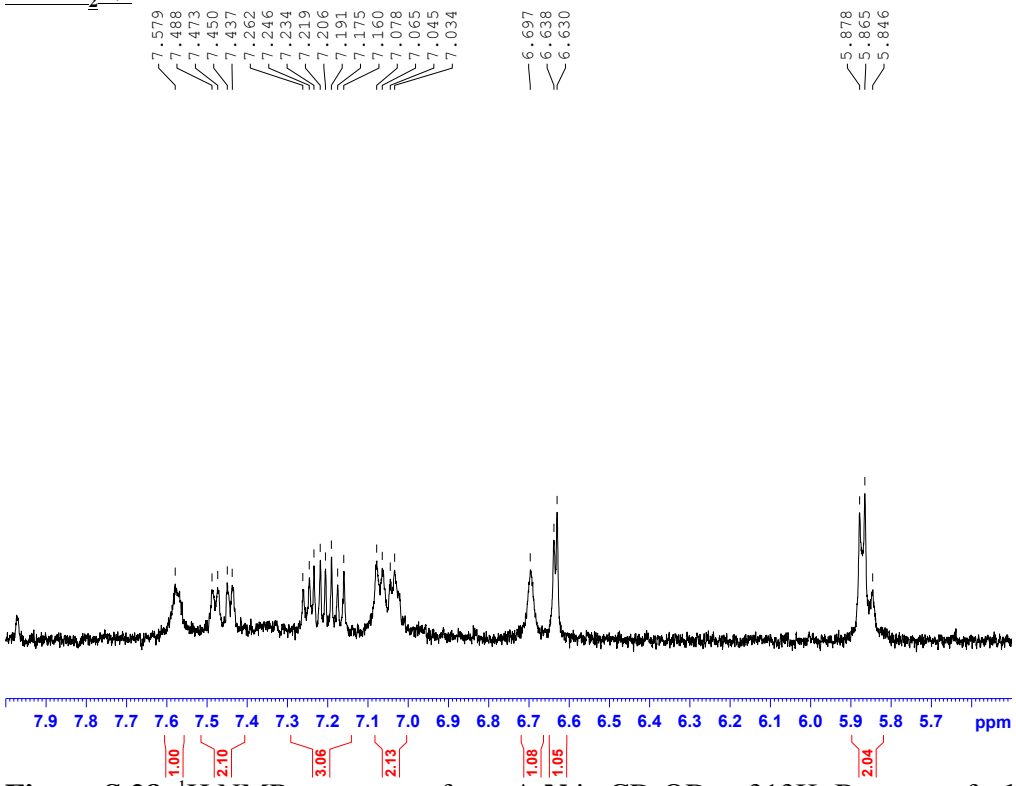

Figure S 28. ^{1}H NMR spectrum of *rac*-**A_2N** in CD_3OD at 313K. Because of a lack of symmetry in the macrocycle, there is significant overlap of proton peaks that complicate their assignment. Therefore, exact proton assignments were not made.

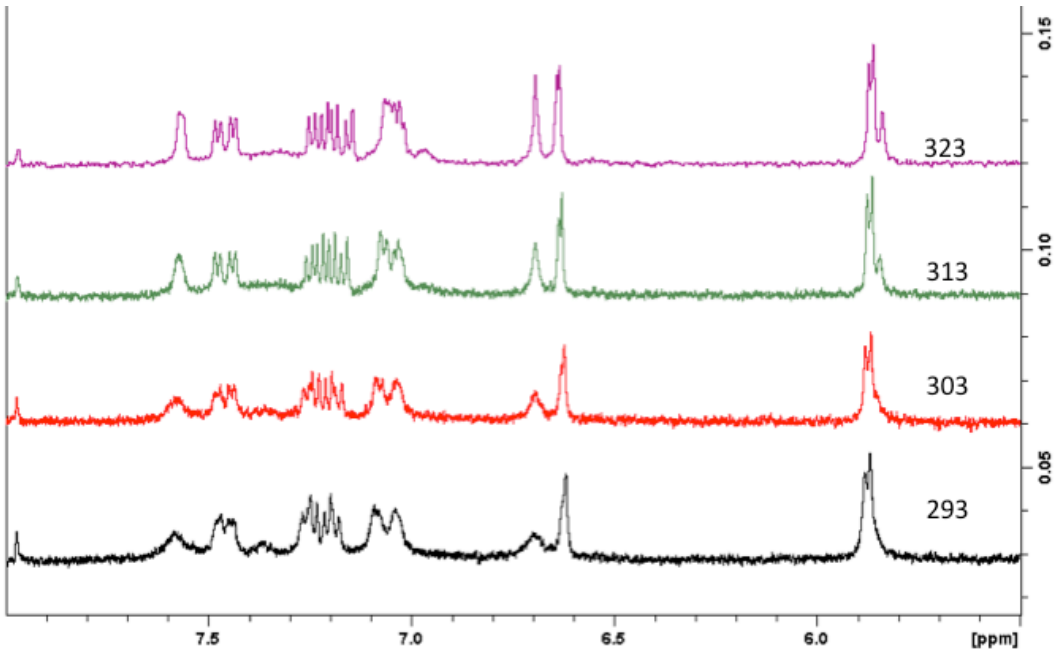

Figure S 29. Impact of temperature on the ^{1}H NMR spectrum of *rac*-**A_2N** in CD_3OD.

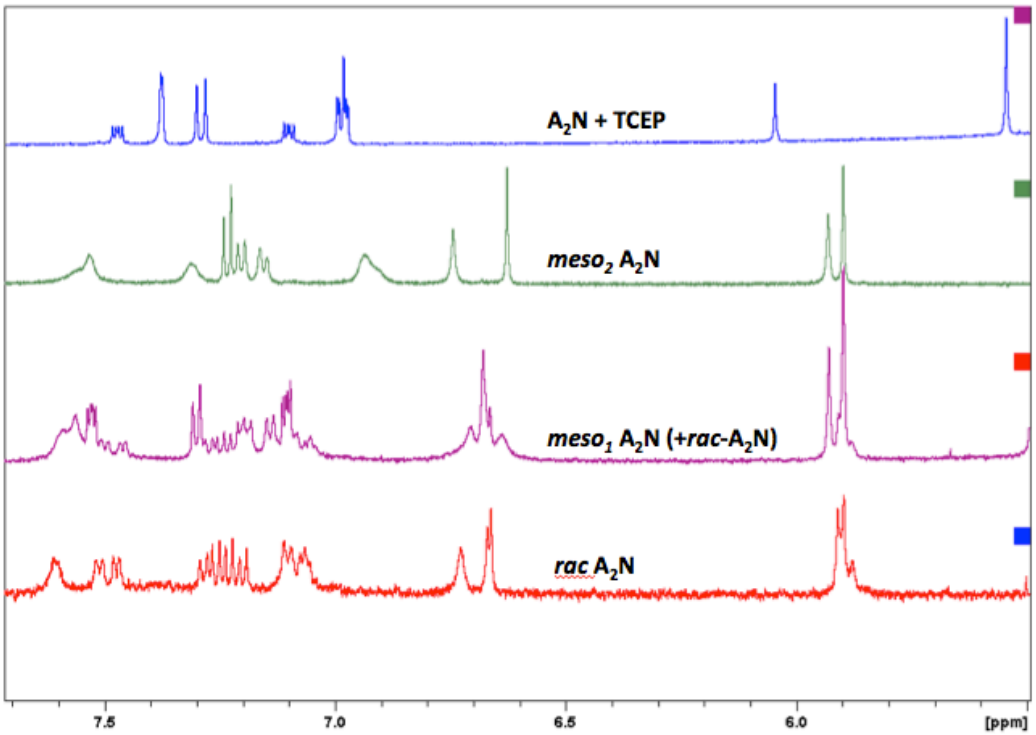

Figure S 30. Overlaid ^{1}H spectra of the three isomers of **A_2N** in CD_3OD, as well as the spectrum that results when any of the isomers are treated with the reducing agent TCEP in CD_3OD.

Extinction Coefficient Determination of A_2N and A_2B. To be able to rapidly determine the concentration of **A_2N** and **A_2B**, extinction coefficients were determined from mixtures of the respective isomers of each receptor. After purifying by RP-HPLC using NH_4OAc as the mobile phase additive, the receptors were lyophilized for three to five days to ensure complete removal of the volatile NH_4OAc salts. The dried receptors were then dissolved into anhydrous methanol and filtered with a .33 μm filter to remove any remaining salts. The methanol was evaporated and the receptor was further dried under vacuum. After accurately determining the mass, stock solutions were prepared in 10 mM sodium borate buffer (pH 8.5). An aliquot of each stock was diluted to 0.372 mM for **A_2N** and 0.912 mM for **A_2B**, and serial dilutions (1:4 for **A_2N** and 1:3 for **A_2B**) were performed to give 10 concentrations. The absorbance at 300 nm (**A_2N**) and 315 nm (**A_2B**) was measured for each concentration, and the absorbance was then plotted against the concentration (Figure S31). The extinction coefficient of **A_2N** was determined from linear regression of this data to be 11,665 $M^{-1}cm^{-1}$ and that of **A_2B** to be 5367 $M^{-1}cm^{-1}$.

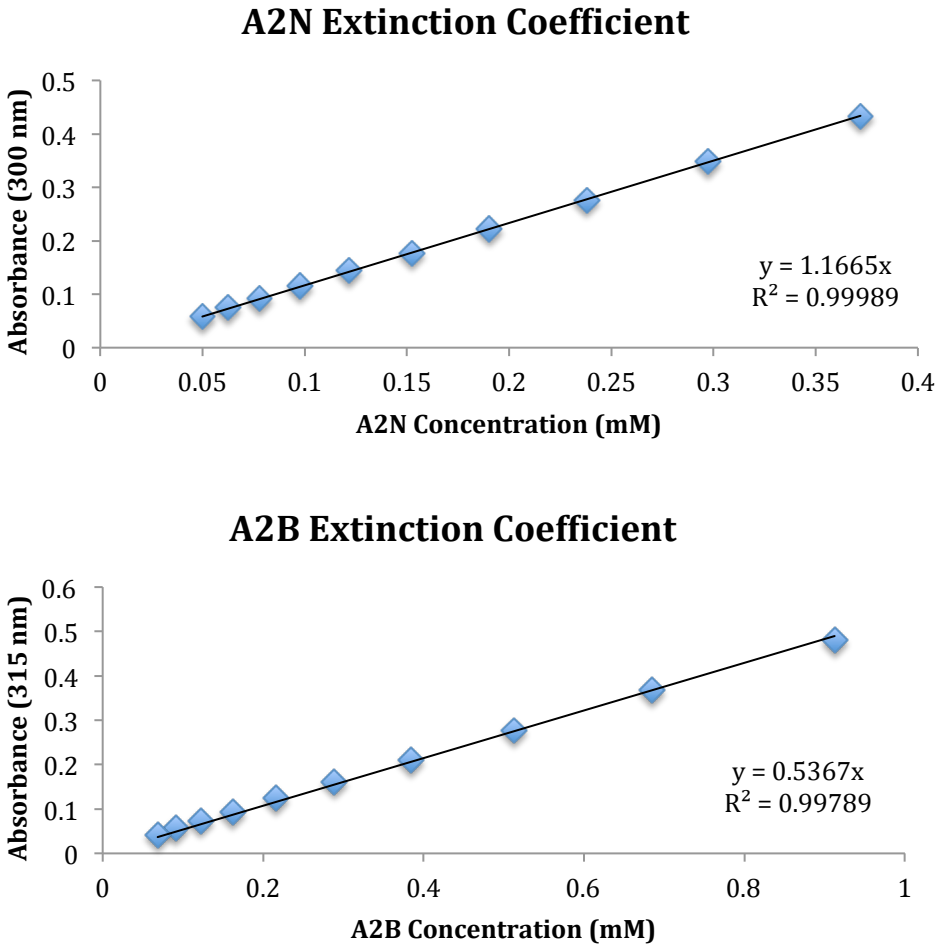

Figure S 31. Extinction coefficient determination of **A_2N** (top) and **A_2B** (bottom). The extinction coefficient was determined as the slope of the line of regression.

NMR Binding Experiments. Binding experiments were carried out with *meso*$_2$-**A$_2$N**, *rac*-**A$_2$B**, and the short dipeptide Ac-Kme$_3$G-NH$_2$. All experiments were carried out in borate buffered D_2O at pH 8.67. Samples were prepared by dissolving lyophilized receptor into 400 uL of a 600 uM solution of the peptide in buffer. Concentration measurements were made for the peptide using DSS as an internal standard. To determine the concentration of the receptor, the absorbance was determined on a nanodrop using the 600 uM peptide solution as a blank.

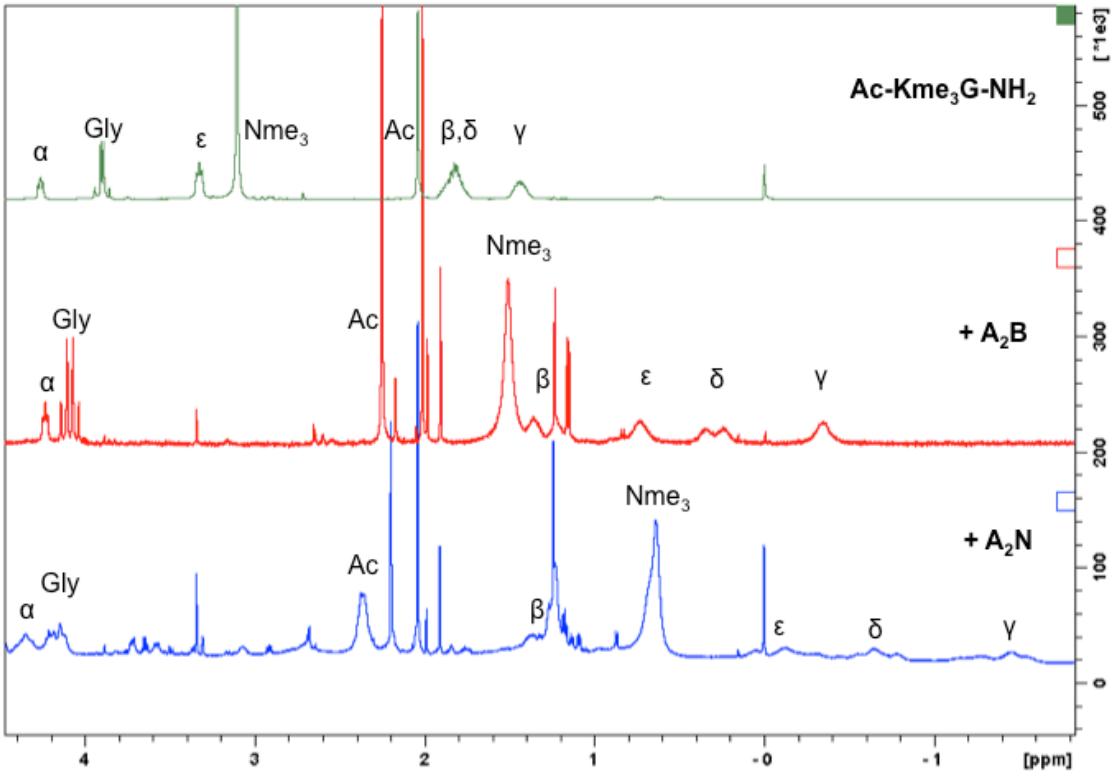

Figure S 32. Overlaid NMR spectra of the peptide Ac-Kme$_3$G-NH$_2$ alone (top) and in the presence of excess *rac*-**A$_2$B** (middle, [Kme$_3$] = 0.60 mM, [**A$_2$B**] = 0.88 mM) or *meso*$_2$-**A$_2$N** (bottom, [Kme$_3$] = 0.55 mM, [**A$_2$N**] = 0.81 mM)

ITC Binding Experiments. Depending on the K_d, titrations were performed with a range of 0.5-3 mM peptide into ~50-200 μM receptor. For situations where binding is weak and the c-value is low (~1), there is a higher degree of error in the binding data. Due to the excessively high concentration of receptor necessary to get accurate numbers in these situations, we are only able to interpret K_d's qualitatively and make no conclusions about trends in ΔH or ΔS. It should be noted that while a one-site binding model is used to fit the ITC data, N-values that deviate from 1 are observed in many situations. We contribute these deviations both to error in the concentration determination of the receptors that arises from the difficulty in determining accurate extinction coefficients by mass and to the complexity of the binding interaction of the receptors to Kme_X when the surrounding peptide sequence can influence the interaction.

Table S1 shows the data for *meso*$_2$-A2N binding to the various methylation states of Arg8. Table S2 shows the data for the two minor isomers of **A_2N** binding to the various methylation states of Lys9. The data for binding to *meso*$_2$-**A_2N** has also been included in table S2 for comparison. Generally, the affinities and selectivities of *rac*-**A_2N** and *meso*$_1$-**A_2N** (both used as mixtures wherein they were the predominant isomer, due to purification challenges) are weaker and show a similar trend to *meso*$_2$-**A_2N**. This is presumed to be due to a difference in the size of the binding pockets, which contributes to complementarity for the methylated Lys guests.

Table S 1. ITC binding data for the binding of *meso*$_2$-**A_2N** to H3 peptides containing different methylation states of Arg. All titrations were performed at 26 °C in 10 mM sodium borate buffer (pH 8.5).

Entry	Peptide	Charge	K_d [b] (uM)	ΔG [b] (kcal/mol)	ΔH [b] (kcal/mol)	TΔS [b] (kcal/mol)
1	H3 aR8me$_2$	+2	16 ± 1	-6.5 ± 0.7	-9.9 ± 0.5	-3.4 ± 0.5
2	H3 sR8me$_2$	+2	68 ± 2	-5.7 ± 0.2	-9.8 ± 0.1	-4.1 ± 0.1
3	H3 sR8me	+2	44 ± 2	-6.0 ± 0.2	-9.6 ± 0.1	-3.6 ± 0.2
4	H3 R8	+2	10.5 ± 0.9	-6.8 ± 0.4	-7.3 ± 0.3	-0.5 ± 0.3

[a] Conditions: 26 °C in 10 mM borate buffer, pH 8.5. [b] Errors are from averages.

Table S 2. ITC binding data for the binding of each of the **A_2N** isomers to various H3 peptides. All titrations were performed at 26 °C in 10 mM sodium borate buffer (pH 8.5).

Entry	Receptor	Peptide	Charge	K_d [b] (uM)	ΔG [b] (kcal/mol)	ΔH [b] (kcal/mol)	$T\Delta S$ [b] (kcal/mol)
1	m_2-A_2N	H3 K9me$_3$	+2	0.30 ± 0.04	-8.9 ± 0.8	-12.0 ± 0.5	-3.1 ± 0.5
2	m_2-A_2N	H3 K9me$_2$	+2	4.1 ± 0.5	-7.4 ± 0.5	-12.5 ± 0.4	-5.1 ± 0.4
3	m_2-A_2N	H3 K9me	+2	40 ± 4	-6.0 ± 0.7	-12.0 ± 0.5	-6.0 ± 0.5
4	m_2-A_2N	H3 K9	+2	10.5 ± 0.9	-6.8 ± 0.4	-7.3 ± 0.3	-0.5 ± 0.3
5	m_2-A_2N	H3 R8G-K9me$_3$	+1	1.3 ± 0.2	-8.1 ± 0.8	-13.4 ± 0.5	-5.3 ± 0.6
6	m_2-A_2N	H3 R8G-K9	+1	362 ± 32	-4.76 ± 0.07	-	-
7	m_2-A_2N	H3 R8-K9G	+1	307 ± 136	-4.8 ± 0.3	-	-
8	m_2-A_2N	H3 R8G-K9G	0	> 1000	> -3.8	-	-
9	m_1-A_2N[c]	H3 K9me$_3$	+2	1.19 ± 0.09	-8.10 ± 0.04	-10.83 ± 0.03	-2.72 ± 0.04
10	m_1-A_2N[c]	H3 K9me$_2$	+2	7.5 ± 0.5	-7.01 ± 0.08	-12.1 ± 0.2	-5.0 ± 0.2
11	m_1-A_2N[c]	H3 K9me	+2	33 ± 4	-6.13 ± 0.08	-12.64 ± 0.05	-6.5 ± 0.1
12	m_1-A_2N[c]	H3 K9	+2	13 ± 1	-6.68 ± 0.05	-7.8 ± 0.3	-1.1 ± 0.3
13	m_1-A_2N[c]	H3 R8G-K9me$_3$	+1	3.4 ± 1.3	-7.5 ± 0.2	-11.6 ± 0.2	-4.13 ± 0.06
14	m_1-A_2N[c]	H3 R8G-K9	+1	149 ± 3	-5.23 ± 0.01	-	-
15	m_1-A_2N[c]	H3 R8-K9G	+1	171 ± 18	-5.15 ± 0.06	-	-
16	m_1-A_2N[c]	H3 R8G-K9G	0	> 2000	> -3.5	-	-
17	r-A_2N[c]	H3 K9me$_3$	+2	1.3 ± 0.2	-8.04 ± 0.09	-10.53 ± 0.04	-2.5 ± 0.1
18	r-A_2N[c]	H3 K9me$_2$	+2	7.7 ± 1.0	-6.99 ± 0.08	-11.2 ± 0.4	-4.2 ± 0.5
19	r-A_2N[c]	H3 K9me	+2	35 ± 5	-6.09 ± 0.08	-12.3 ± 0.5	-6.2 ± 0.5
20	r-A_2N[c]	H3 K9	+2	13.5 ± 0.9	-6.65 ± 0.04	-7.3 ± 0.7	-0.6 ± 0.8
21	r-A_2N[c]	H3 R8G-K9me$_3$	+1	4.3 ± 2.4	-7.3 ± 0.3	-10.7 ± 0.2	-3.4 ± 0.3
22	r-A_2N[c]	H3 R8G-K9	+1	217 ± 9	-5.01 ± 0.02	-	-
23	r-A_2N[c]	H3 R8-K9G	+1	210 ± 30	-5.03 ± 0.08	-	-
24	r-A_2N[c]	H3 R8G-K9G	0	> 2000	> -3.7	-	-

[a] Conditions: 26 °C in 10 mM borate buffer, pH 8.5. [b] Errors are from averages. [c] *rac*-**A_2N** and *meso*$_1$-**A_2N** are used as mixtures that they represent the major component of, due to purification challenges.

meso$_2$-**A$_2$N** + H3 K9me$_X$:

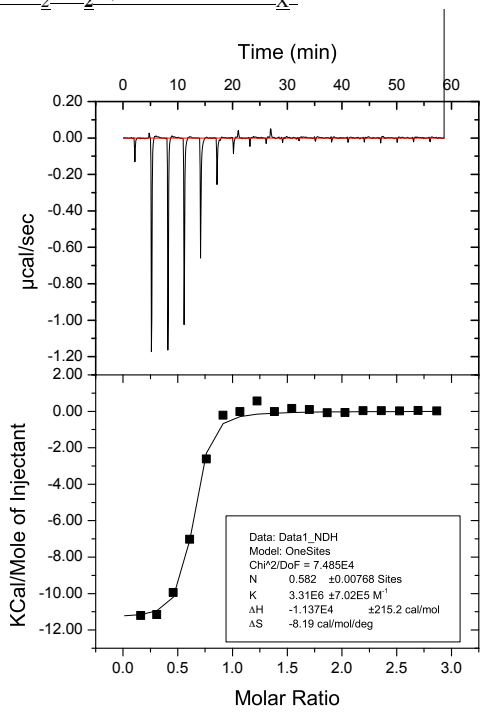

Figure S 33. One of three trials of H3 K9me$_3$ (WGGG-QTARKme$_3$STG-NH$_2$) (575 µM) titrated into *meso*$_2$-**A$_2$N** (39 µM) at 26 ºC in 10 mM borate buffer, pH 8.5.

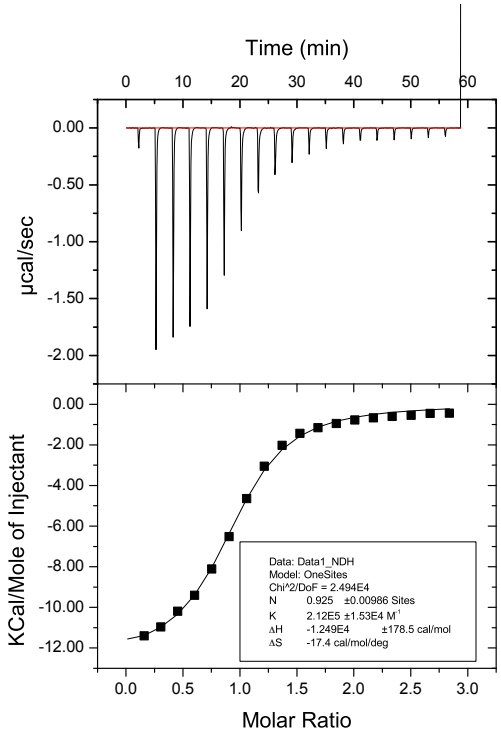

Figure S 34. One of three trials of H3 K9me$_2$ (WGGG-QTARKme$_2$STG-NH$_2$) (938 µM) titrated into *meso*$_2$-**A$_2$N** (63 µM) at 26 ºC in 10 mM borate buffer, pH 8.5.

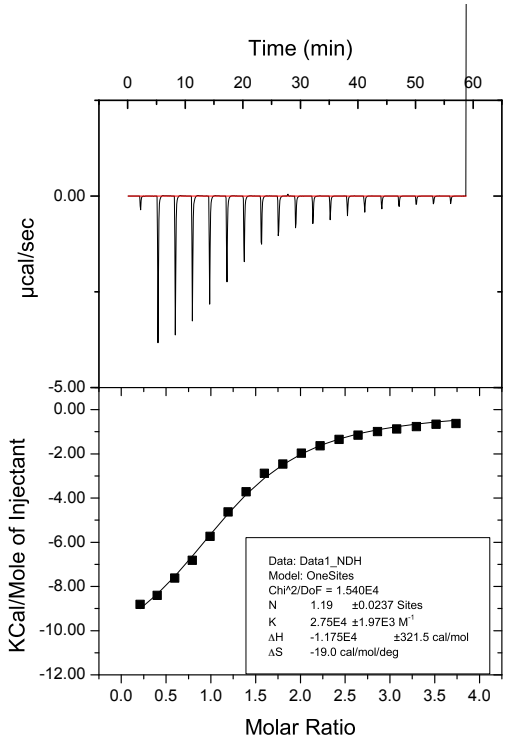

Figure S 35. One of three trials of H3 K9me (WGGG-QTARKmeSTG-NH_2) (2.32 mM) titrated into *meso*$_2$-$\mathbf{A_2N}$ (119 µM) at 26 ºC in 10 mM borate buffer, pH 8.5.

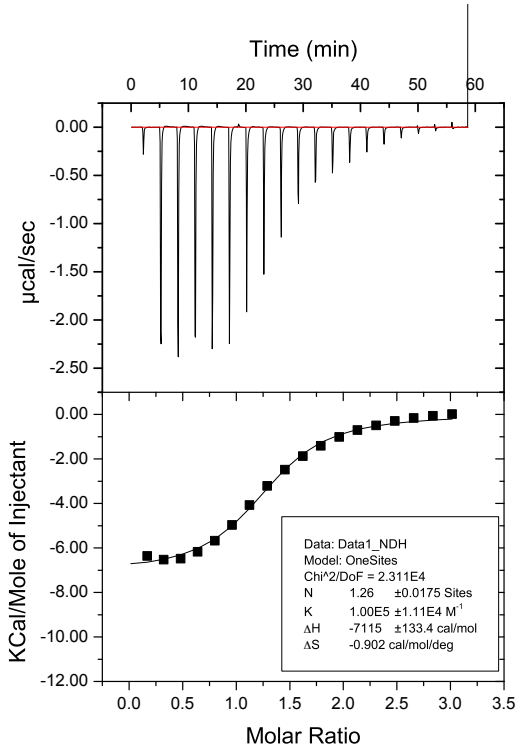

Figure S 36. One of three trials of H3 K9 (WGGG-QTARKSTG-NH_2) (2.06 mM) titrated into *meso*$_2$-$\mathbf{A_2N}$ (131 µM) at 26 ºC in 10 mM borate buffer, pH 8.5.

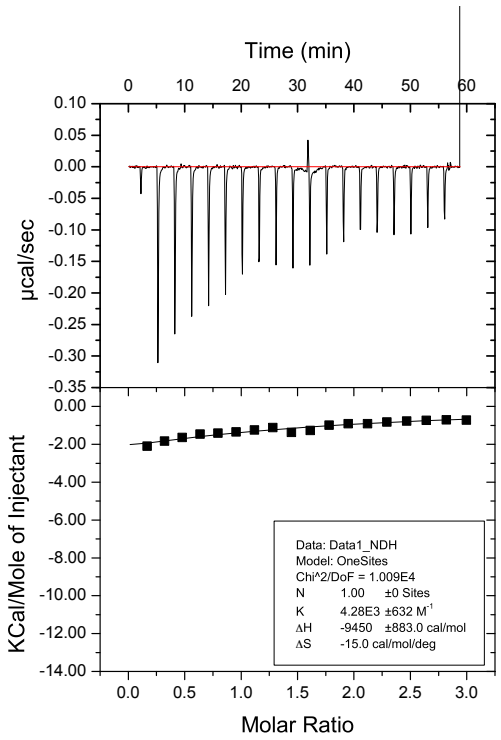

Figure S 37. One of three trials of H3 R8-K9G (WGGG-QTARGSTG-NH_2) (990 µM) titrated into *meso*$_2$-$\mathbf{A_2N}$ (63 µM) at 26 ºC in 10 mM borate buffer, pH 8.5.

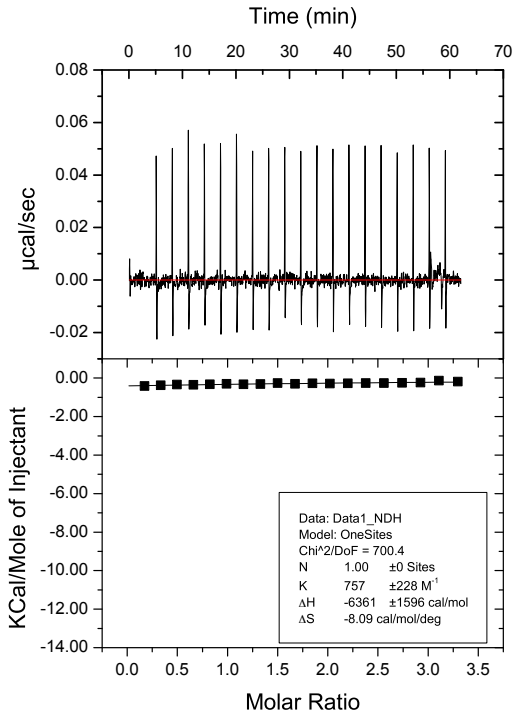

Figure S 38. One of two trials of H3 R8G-K9G (WGGG-QTAGGSTG-NH_2) (1.44 mM) titrated into *meso*$_2$-$\mathbf{A_2N}$ (89 µM) at 26 ºC in 10 mM borate buffer, pH 8.5.

meso$_2$-**A$_2$N** + H3 R8GK9me$_X$:

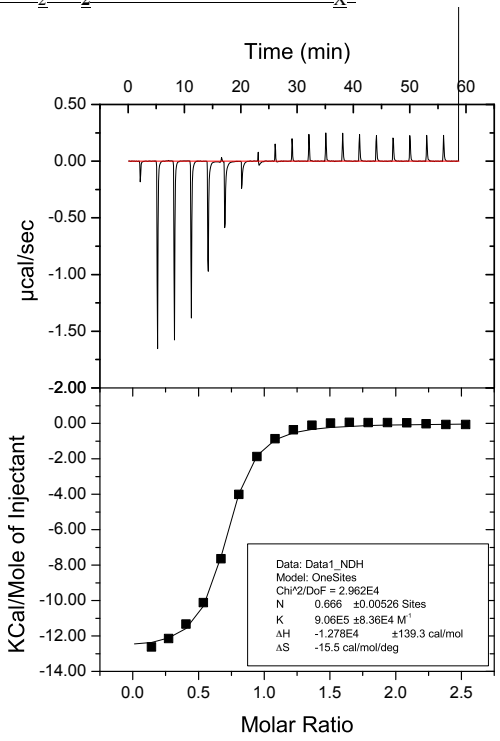

Figure S 39. One of three trials of H3 R8G-K9me$_3$ (WGGG-QTAGKme$_3$STG-NH$_2$) (837 µM) titrated into *meso*$_2$-**A$_2$N** (63 µM) at 26 ºC in 10 mM borate buffer, pH 8.5.

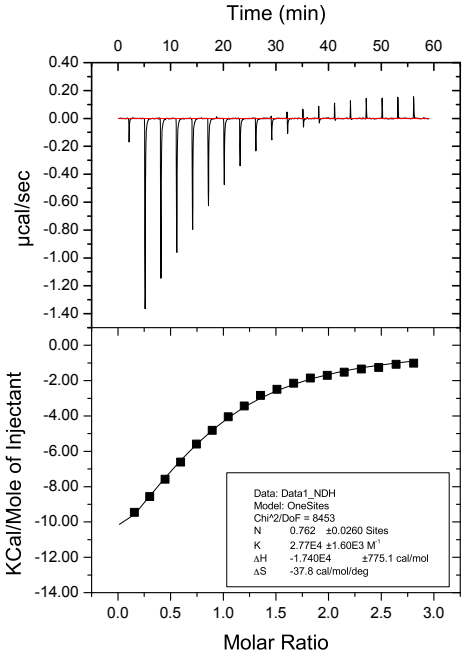

Figure S 40. One of three trials of H3 R8G-K9me$_2$ (WGGG-QTAGKme$_2$STG-NH$_2$) (980 µM) titrated into *meso*$_2$-**A$_2$N** (67 µM) at 26 ºC in 10 mM borate buffer, pH 8.5.

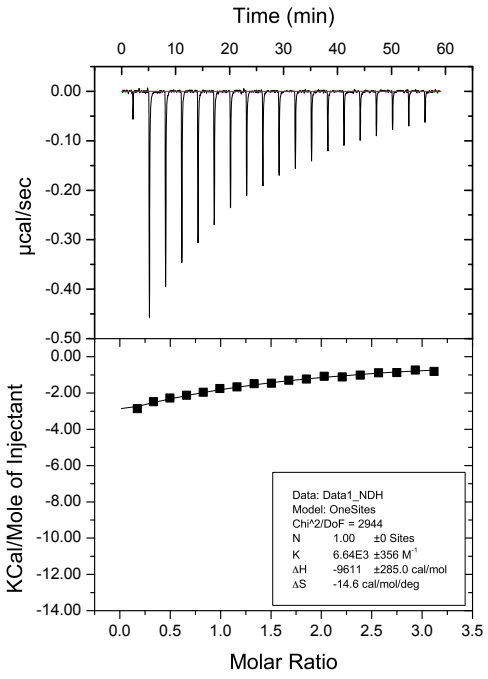

Figure S 41. One of three trials of H3 R8G-K9me (WGGG-QTAGKmeSTG-NH_2) (1.04 mM) titrated into *meso*$_2$-$\mathbf{A_2N}$ (64 µM) at 26 ºC in 10 mM borate buffer, pH 8.5.

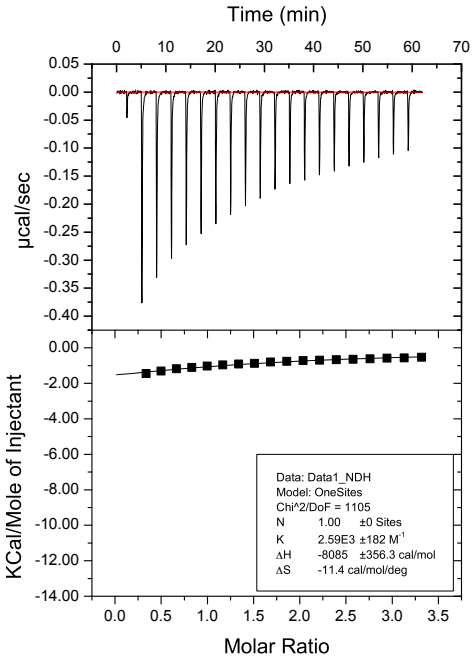

Figure S 42. One of three trials of H3 R8G-K9 (WGGG-QTAGKSTG-NH_2) (1.45 mM) titrated into *meso*$_2$-$\mathbf{A_2N}$ (89 µM) at 26 ºC in 10 mM borate buffer, pH 8.5.

rac-**A$_2$B** + H3 K9me$_X$:

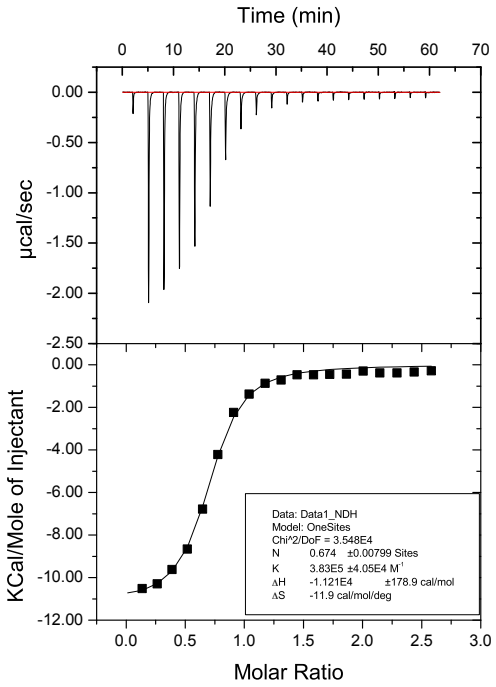

Figure S 43. One of three trials of H3 K9me$_3$ (WGGG-QTARK me$_3$STG-NH$_2$) (1.08 mM) titrated into *rac*-**A$_2$B** (85 µM) at 26 ºC in 10 mM borate buffer, pH 8.5.

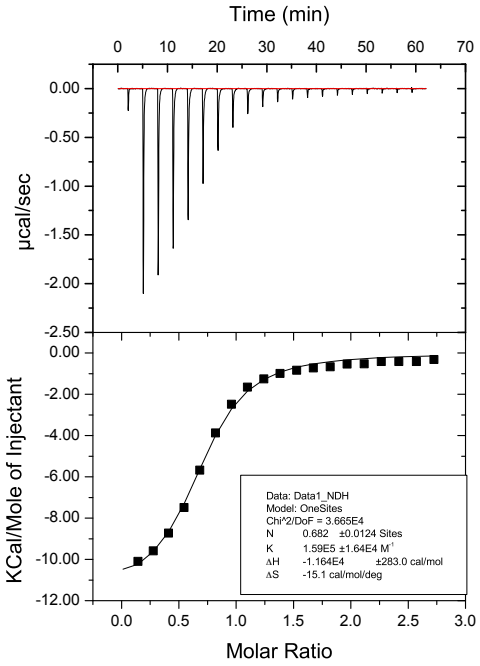

Figure S 44. One of three trials of H3 K9me$_2$ (WGGG-QTARK me$_2$STG-NH$_2$) (1.14 mM) titrated into *rac*-**A$_2$B** (85 µM) at 26 ºC in 10 mM borate buffer, pH 8.5.

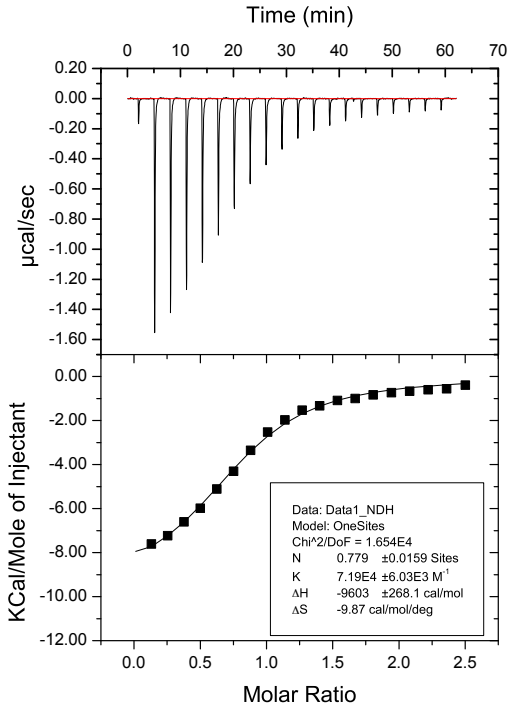

Figure S 45. One of three trials of H3 K9me (WGGG-QTARK meSTG-NH_2) (1.07 mM) titrated into *rac*-$\mathbf{A_2B}$ (87 µM) at 26 ºC in 10 mM borate buffer, pH 8.5.

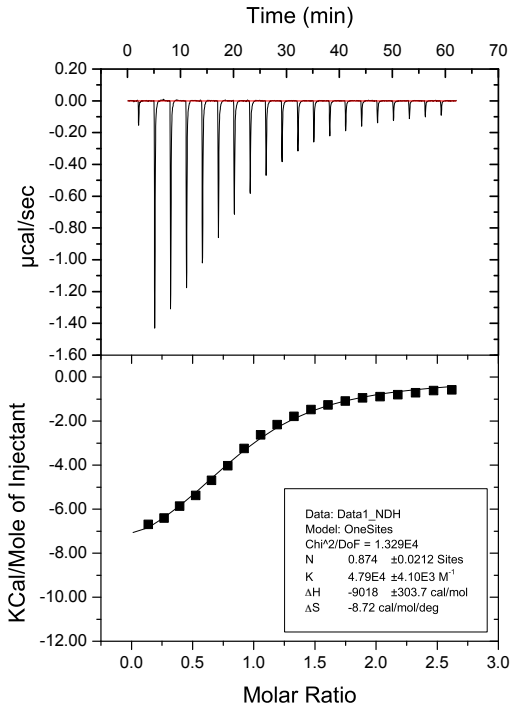

Figure S 46. One of three trials of H3 K9 (WGGG-QTARKSTG-NH_2) (1.12 mM) titrated into *rac*-$\mathbf{A_2B}$ (87 µM) at 26 ºC in 10 mM borate buffer, pH 8.5.

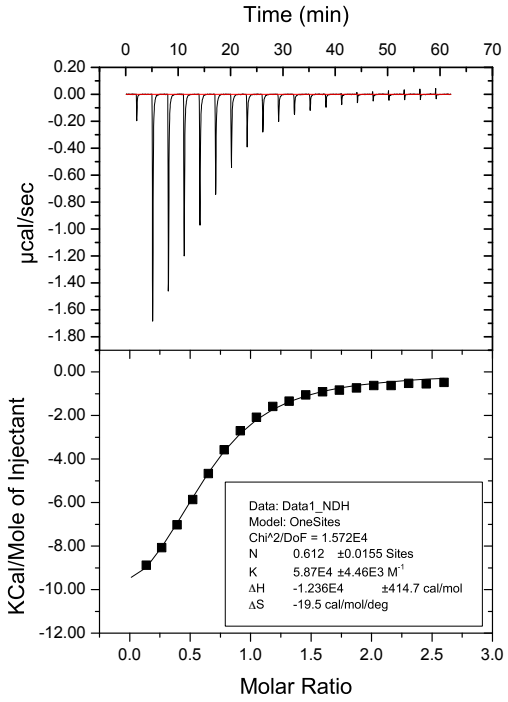

Figure S 47. One of three trials of H3 R8G-K9me$_3$ (WGGG-QTAGK me$_3$STG-NH$_2$) (1.16 mM) titrated into *rac*-**A$_2$B** (91 µM) at 26 ºC in 10 mM borate buffer, pH 8.5.

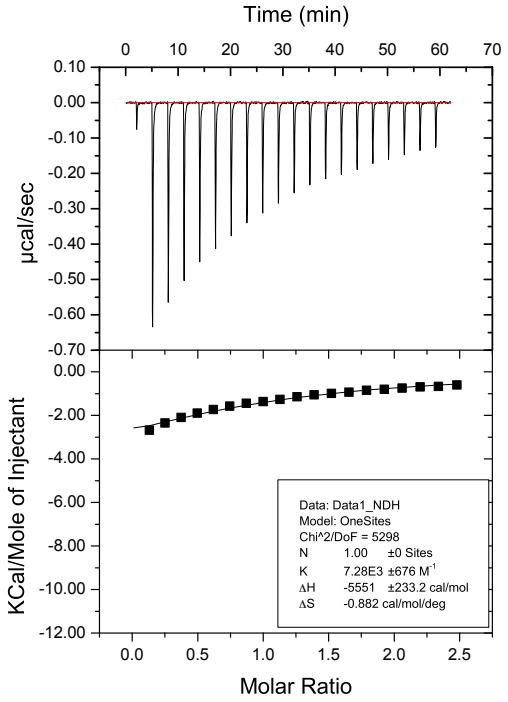

Figure S 48. One of three trials of H3 R8G-K9 (WGGG-QTAGKSTG-NH$_2$) (1.45 mM) titrated into *rac*-**A$_2$B** (119 µM) at 26 ºC in 10 mM borate buffer, pH 8.5.

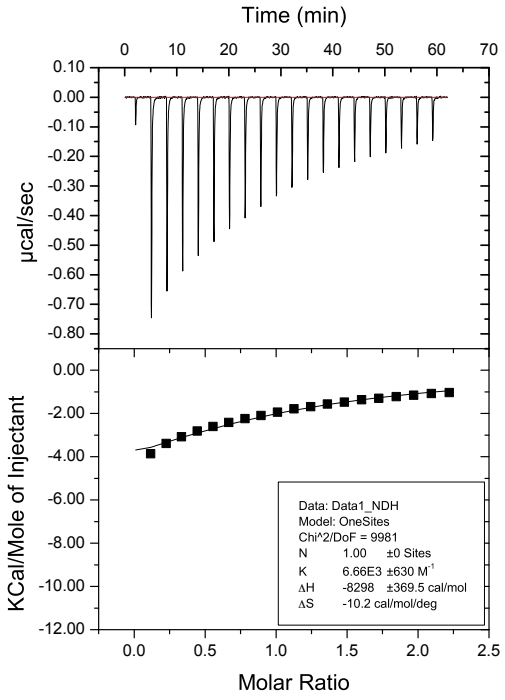

Figure S 49. One of three trials of H3 R8-K9G (WGGG-QTARGSTG-NH_2) (1.32 mM) titrated into *rac*-$\mathbf{A_2B}$ (121 µM) at 26 ºC in 10 mM borate buffer, pH 8.5.

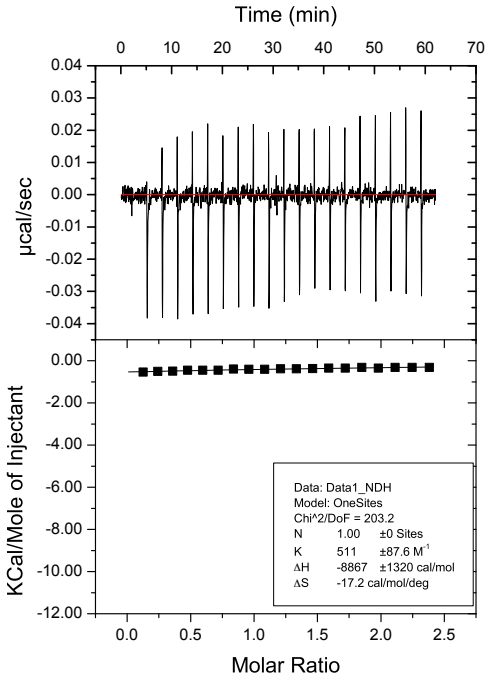

Figure S 50. One of two trials of H3 R8G-K9G (WGGG-QTAGGSTG-NH_2) (1.44 mM) titrated into *rac*-$\mathbf{A_2B}$ (123 µM) at 26 ºC in 10 mM borate buffer, pH 8.5.

meso$_2$-**A$_2$N** + H3 K36me$_X$:

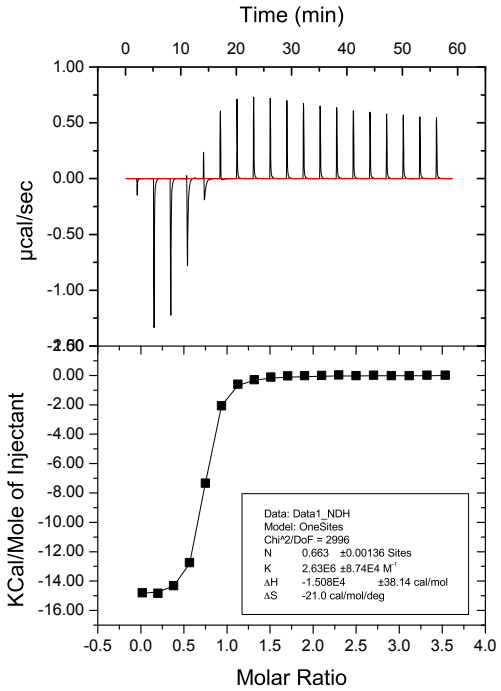

Figure S 51. One of three trials of H3 K36me$_3$ (WGGG-TGGVKme$_3$KPH-NH$_2$) (663 µM) titrated into *meso*$_2$-**A$_2$N** (36 µM) at 26 ºC in 10 mM borate buffer, pH 8.5.

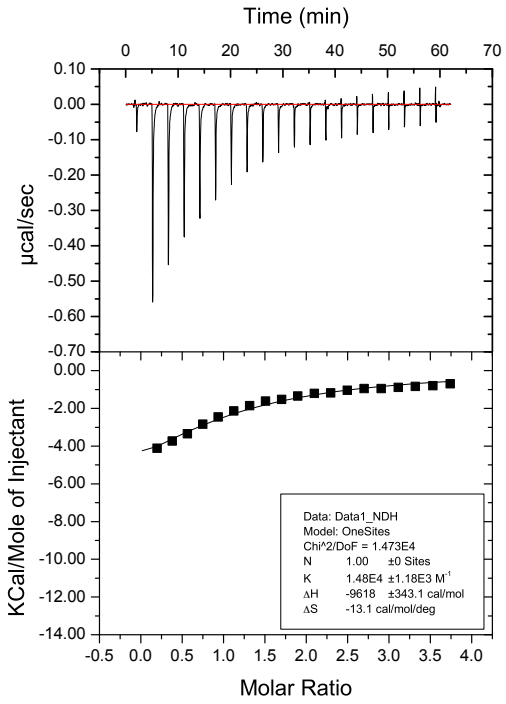

Figure S 52. One of two trials of H3 K36 (WGGG-TGGVKKPH-NH$_2$) (995 µM) titrated into *meso*$_2$-**A$_2$N** (54 µM) at 26 ºC in 10 mM borate buffer, pH 8.5.

meso$_2$-**A$_2$N** + H3 R8me$_X$:

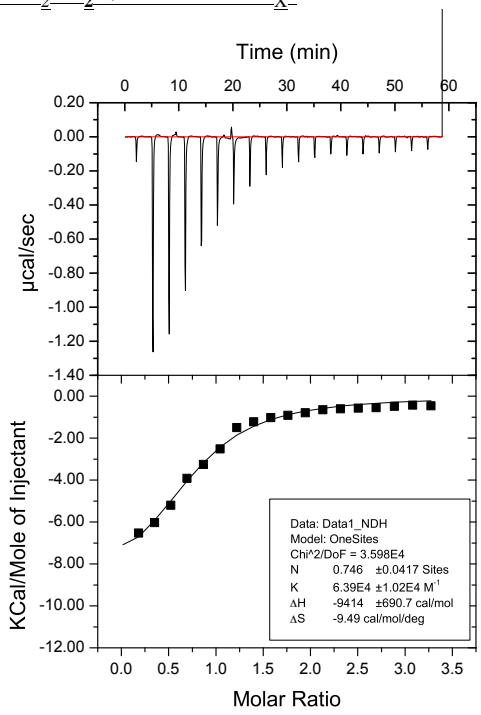

Figure S 53. One of three trials of H3 aR8me$_2$ (WGGG-QTAaRme$_2$KSTG-NH$_2$) (1.11 mM) titrated into *meso*$_2$-**A$_2$N** (65 µM) at 26 ºC in 10 mM borate buffer, pH 8.5.

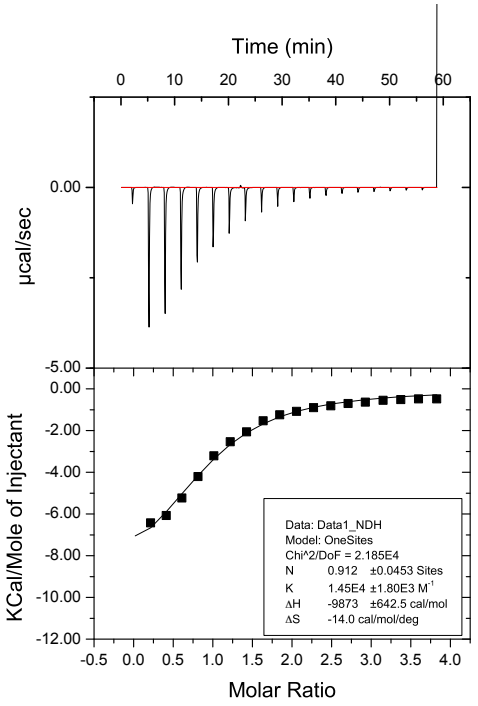

Figure S 54. One of two trials of H3 sR8me$_2$ (WGGG-QTAsRme$_2$KSTG-NH$_2$) (3.83 mM) titrated into *meso*$_2$-**A$_2$N** (192 µM) at 26 ºC in 10 mM borate buffer, pH 8.5.

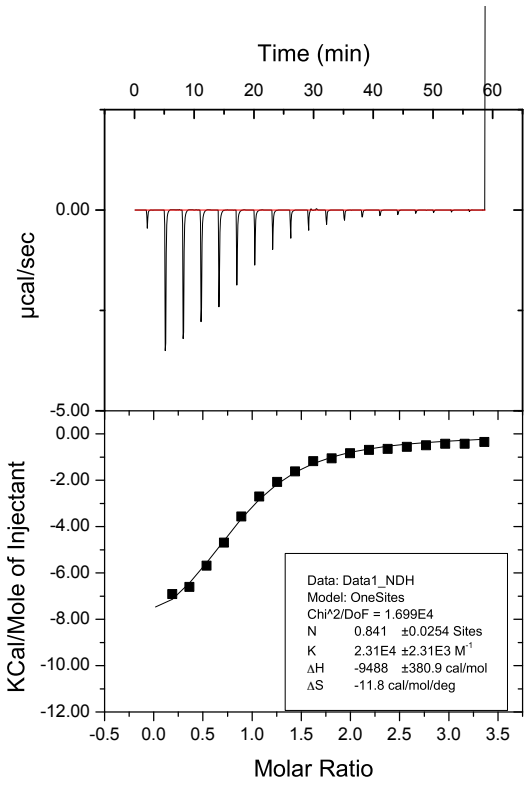

Figure S 55. One of two trials of H3 R8me (WGGG-QTARmeKSTG-NH_2) (3.40 mM) titrated into *meso*$_2$-$\mathbf{A_2N}$ (194 µM) at 26 ºC in 10 mM borate buffer, pH 8.5.

meso$_1$-**A$_2$N** (+ some *rac*-**A$_2$N**) + H3 K9me$_X$:

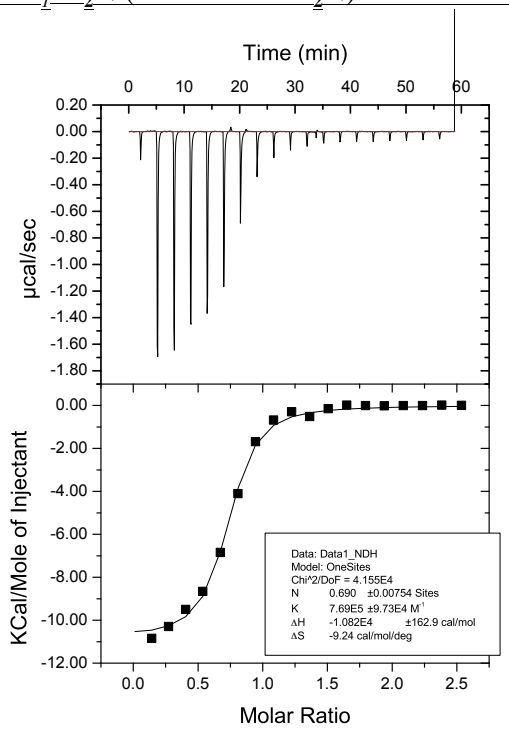

Figure S 56. One of three trials of H3 K9me$_3$ (WGGG-QTARKme$_3$STG-NH$_2$) (937 µM) titrated into *meso*$_1$-**A$_2$N** (71 µM) at 26 ºC in 10 mM borate buffer, pH 8.5.

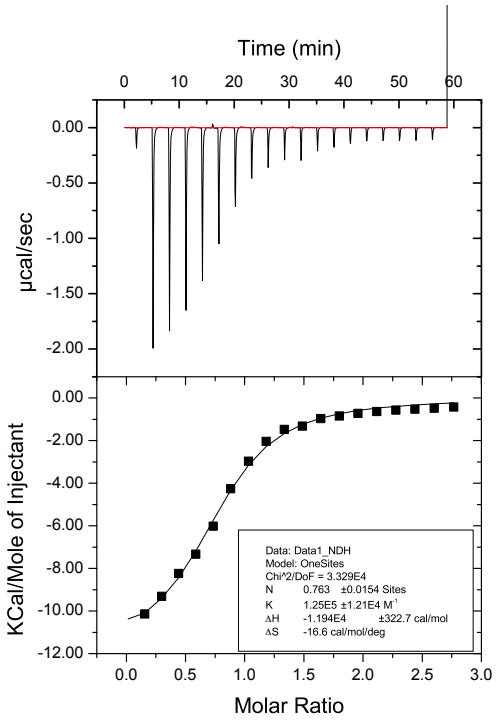

Figure S 57. One of three trials of H3 K9me$_2$ (WGGG-QTARKme$_2$STG-NH$_2$) (1.02 mM) titrated into *meso*$_1$-**A$_2$N** (71 µM) at 26 ºC in 10 mM borate buffer, pH 8.5.

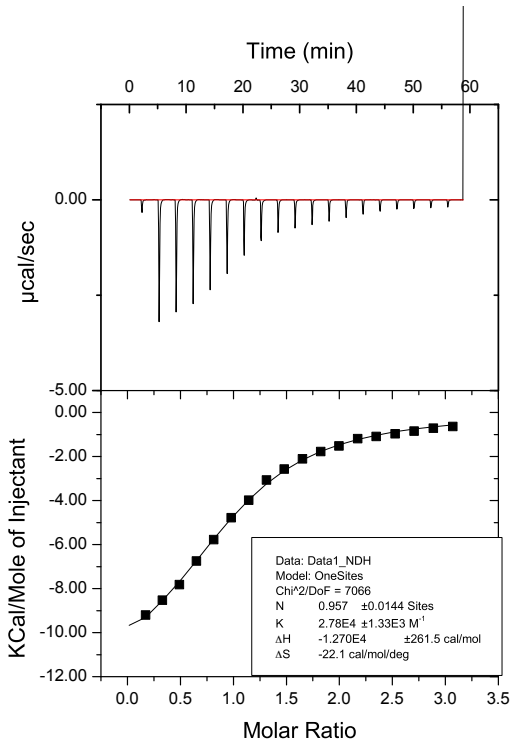

Figure S 58. One of three trials of H3 K9me (WGGG-QTARKmeSTG-NH_2) (1.94 mM) titrated into *meso*$_1$-$\mathbf{A_2N}$ (121 µM) at 26 ºC in 10 mM borate buffer, pH 8.5.

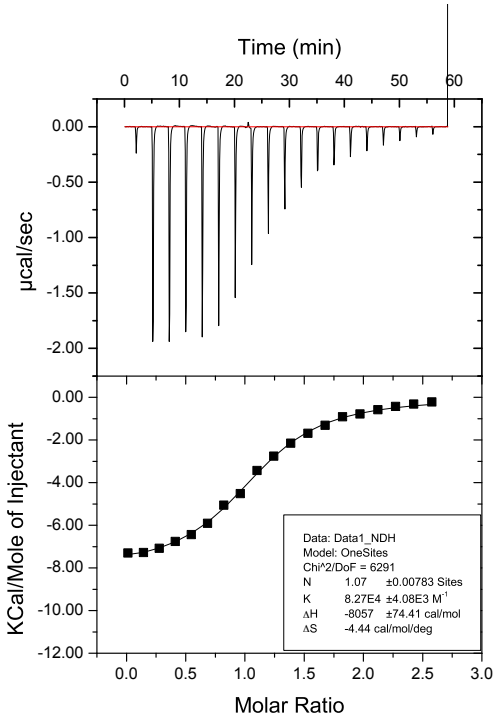

Figure S 59. One of three trials of H3 K9 (WGGG-QTARKSTG-NH_2) (1.63 mM) titrated into *meso*$_1$-$\mathbf{A_2N}$ (121 µM) at 26 ºC in 10 mM borate buffer, pH 8.5.

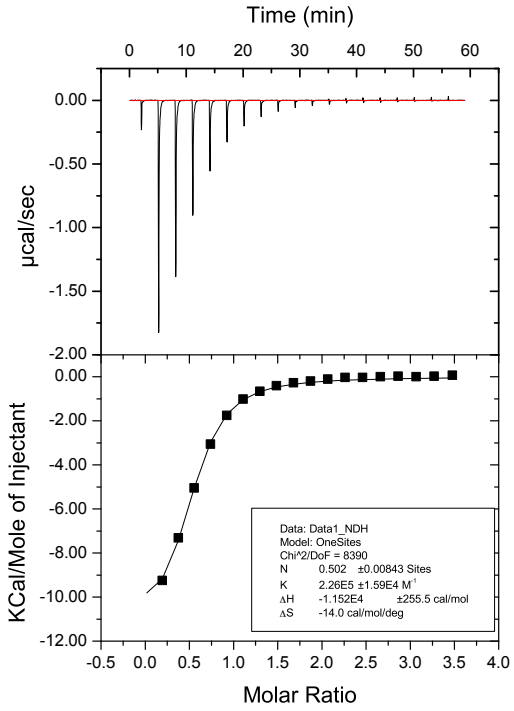

Figure S 60. One of three trials of H3 R8G-K9me$_3$ (WGGG-QTAGKme$_3$STG-NH$_2$) (942 µM) titrated into *meso*$_1$-**A$_2$N** (52 µM) at 26 ºC in 10 mM borate buffer, pH 8.5.

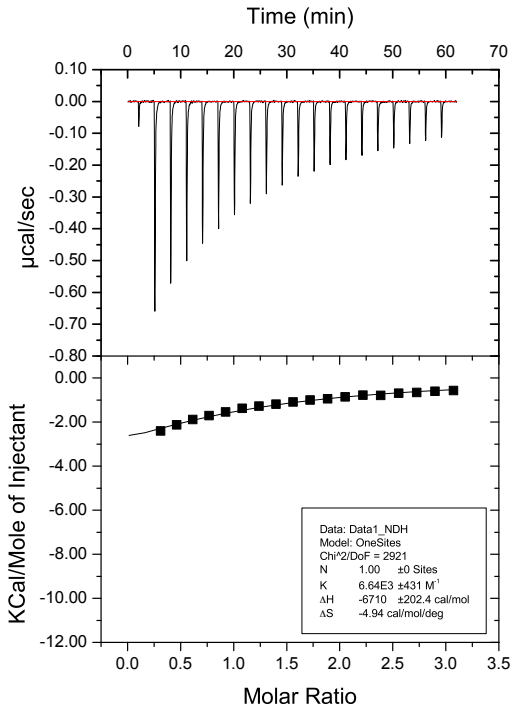

Figure S 61. One of two trials of H3 R8G-K9 (WGGG-QTAGKSTG-NH$_2$) (1.45 mM) titrated into *meso*$_1$-**A$_2$N** (96 µM) at 26 ºC in 10 mM borate buffer, pH 8.5.

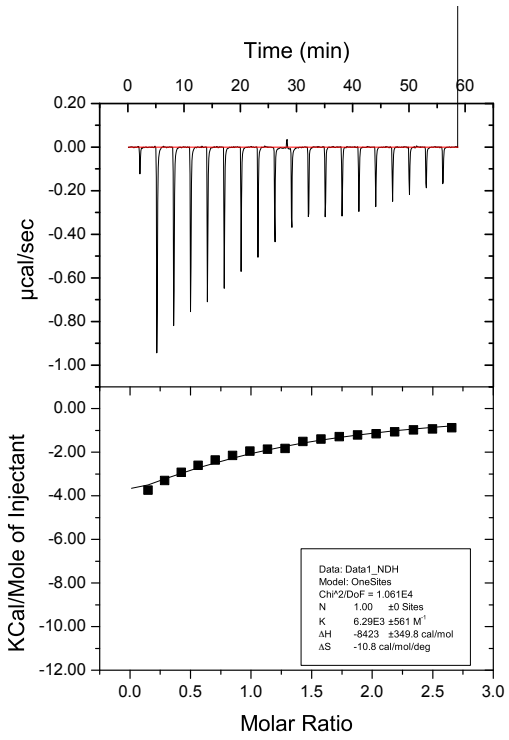

Figure S 62. One of three trials of H3 R8-K9G (WGGG-QTARGSTG-NH_2) (1.69 mM) titrated into *meso*$_1$-$\mathbf{A_2N}$ (123 µM) at 26 ºC in 10 mM borate buffer, pH 8.5.

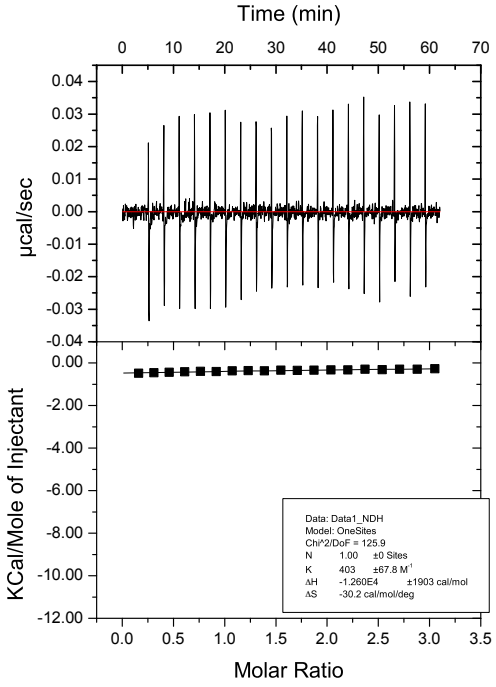

Figure S 63. One of two trials of H3 R8G-K9G (WGGG-QTAGGSTG-NH_2) (1.44 mM) titrated into *meso*$_1$-$\mathbf{A_2N}$ (96 µM) at 26 ºC in 10 mM borate buffer, pH 8.5.

rac-**A$_2$N** (+ some *meso$_1$*-**A$_2$N**) + H3K9me$_X$:

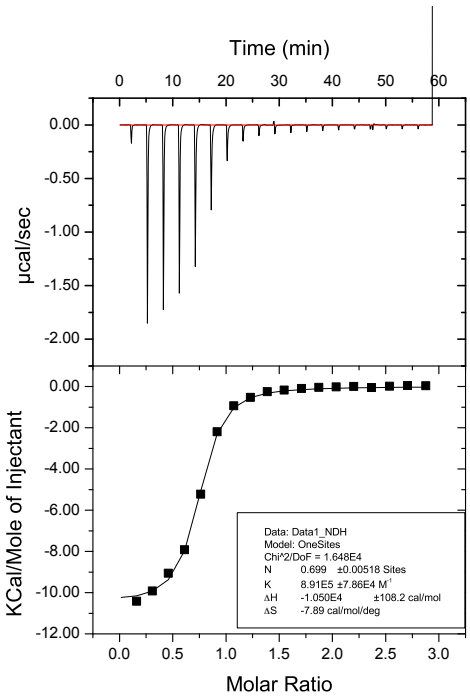

Figure S 64. One of three trials of H3 K9me$_3$ (WGGG-QTARKme$_3$STG-NH$_2$) (937 µM) titrated into *rac*-**A$_2$N** (63 µM) at 26 ºC in 10 mM borate buffer, pH 8.5.

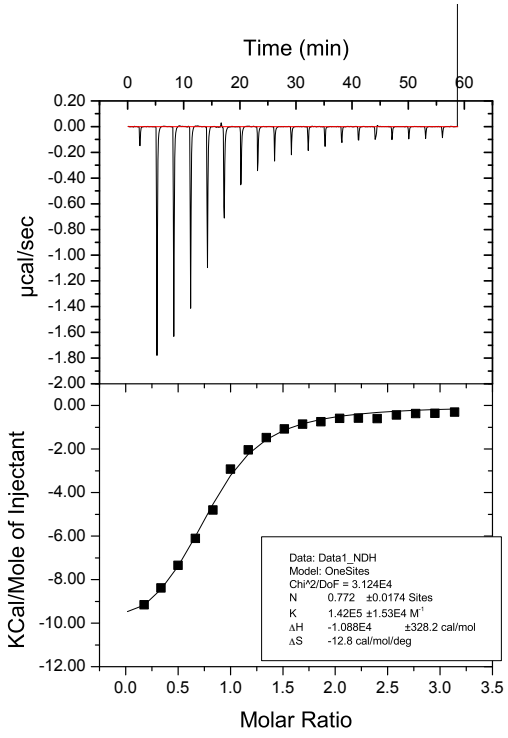

Figure S 65. One of three trials of H3 K9me$_2$ (WGGG-QTARKme$_2$STG-NH$_2$) (1.02 mM) titrated into *rac*-**A$_2$N** (63 µM) at 26 ºC in 10 mM borate buffer, pH 8.5.

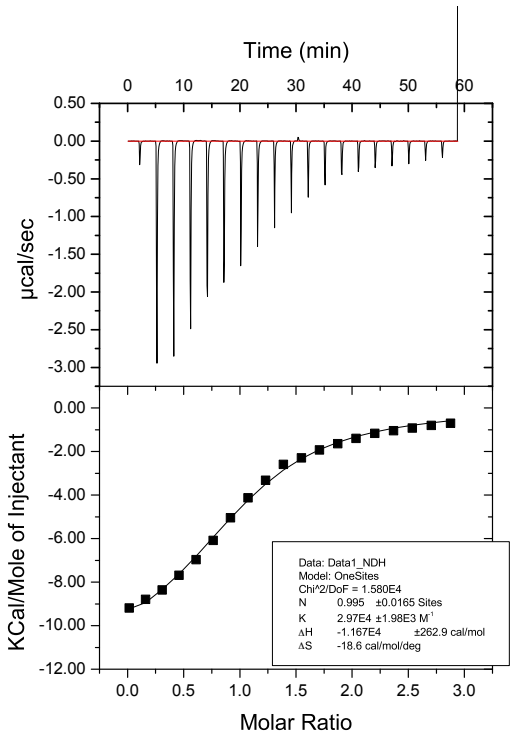

Figure S 66. One of three trials of H3 K9me (WGGG-QTARKmeSTG-NH_2) (1.94 mM) titrated into *rac*-$\mathbf{A_2N}$ (129 µM) at 26 ºC in 10 mM borate buffer, pH 8.5.

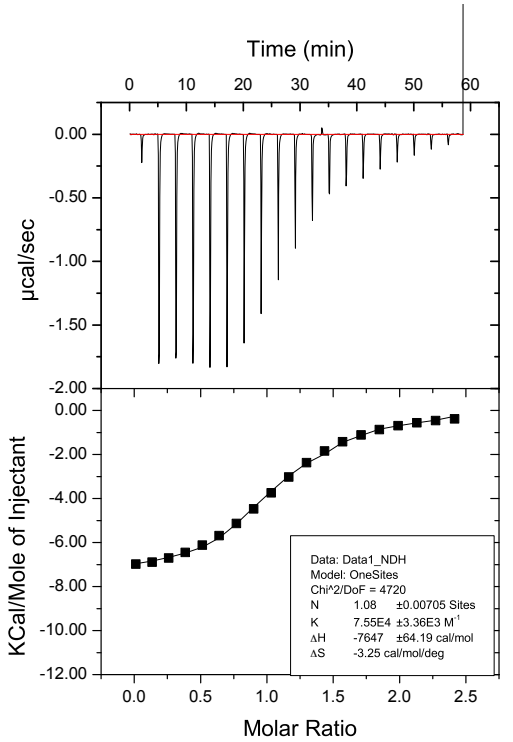

Figure S 67. One of three trials of H3 K9 (WGGG-QTARKSTG-NH_2) (1.63 mM) titrated into *rac*-$\mathbf{A_2N}$ (129 µM) at 26 ºC in 10 mM borate buffer, pH 8.5.

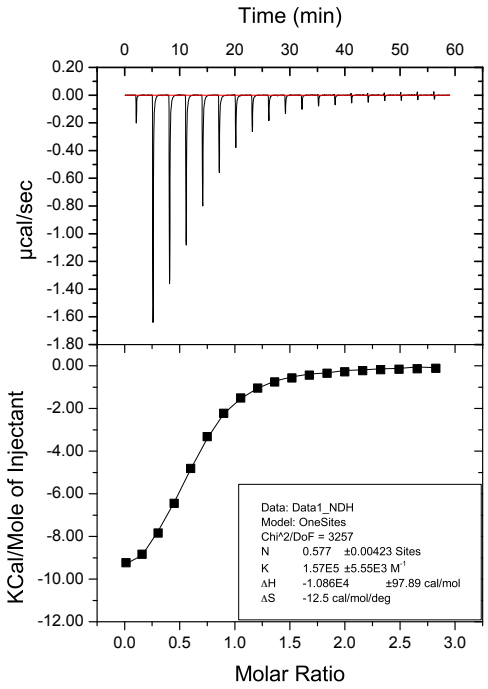

Figure S 68. One of three trials of H3 R8G-K9me$_3$ (WGGG-QTAGKme$_3$STG-NH$_2$) (942 µM) titrated into *rac*-**A$_2$N** (64 µM) at 26 ºC in 10 mM borate buffer, pH 8.5.

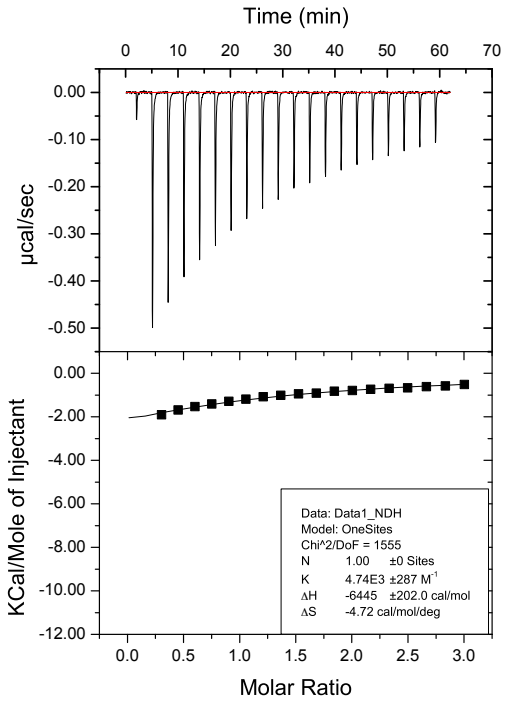

Figure S 69. One of two trials of H3 R8G-K9 (WGGG-QTAGKSTG-NH$_2$) (1.45 mM) titrated into *rac*-**A$_2$N** (98 µM) at 26 ºC in 10 mM borate buffer, pH 8.5.

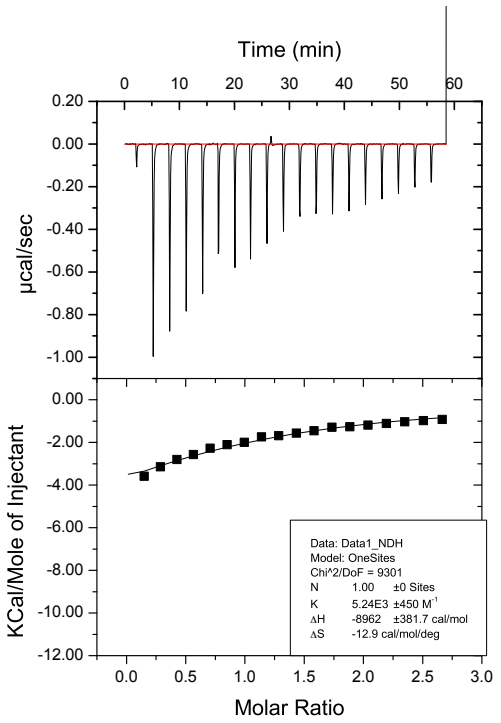

Figure S 70. One of three trials of H3 R8-K9G (WGGG-QTARGSTG-NH_2) (1.69 mM) titrated into *rac*-$\mathbf{A_2N}$ (122 µM) at 26 ºC in 10 mM borate buffer, pH 8.5.

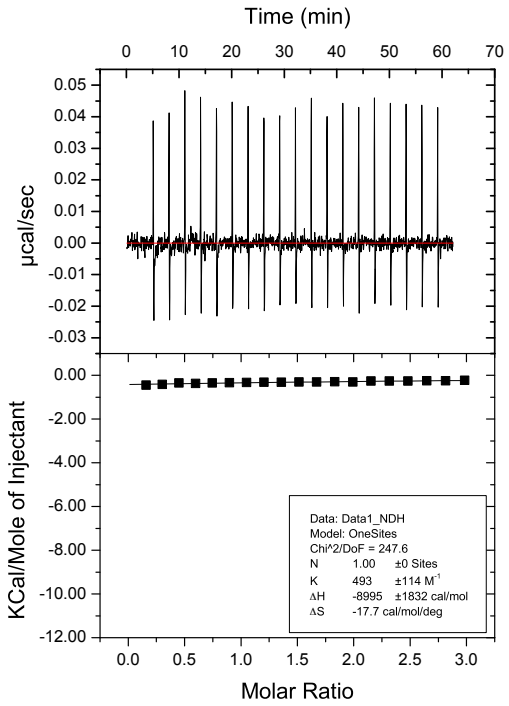

Figure S 71. One of two trials of H3 R8G-K9G (WGGG-QTAGGSTG-NH_2) (1.44 mM) titrated into *rac*-$\mathbf{A_2N}$ (98 µM) at 26 ºC in 10 mM borate buffer, pH 8.5.

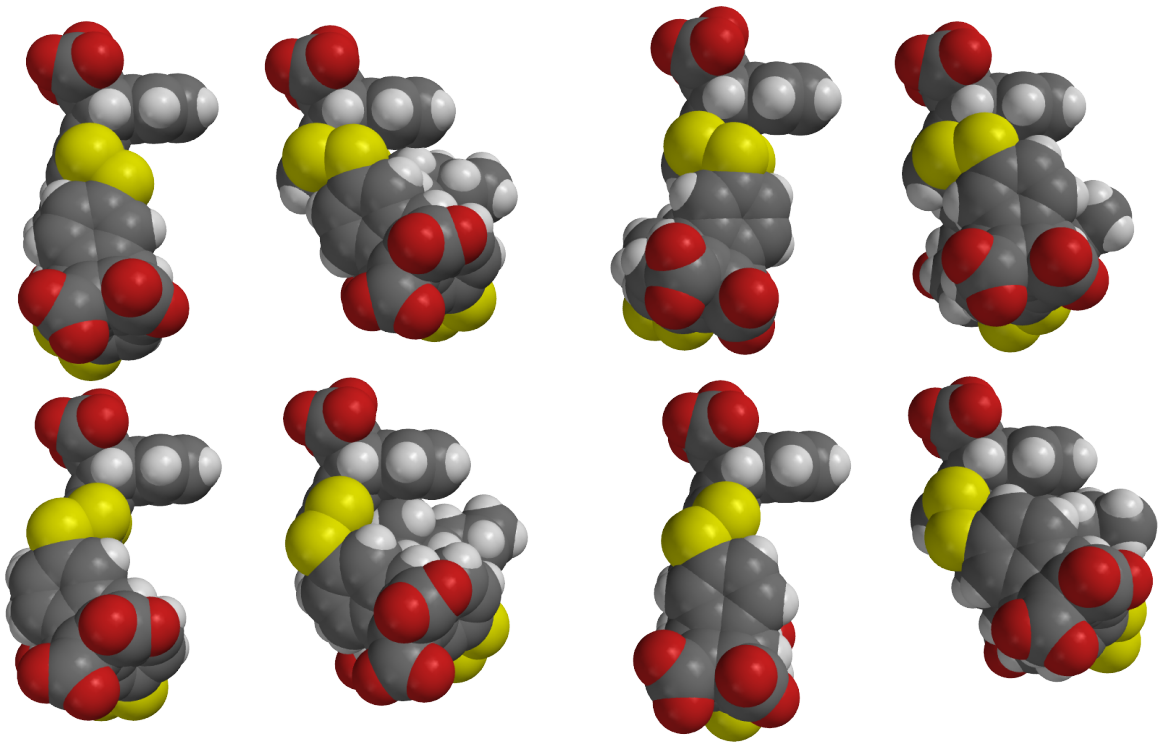

Figure S72. Gas phase minimized structures of meso1-A2N and meso2-A2N in the absence and presence of butyl trimethyl ammonium. As columns from left to right: meso1-A2N (top and bottom: 2 conformations); meso1-A2N bound to butyl trimethyl ammonium (top and bottom: 2 conformations); meso2-A2N (top and bottom: 2 conformations); meso2-A2N bound to butyl trimethyl ammonium (top and bottom: 2 conformations).